Shear Bands

Hans J. Herrmann,
Fernando Alonso-Marroquin
Jan Astrøm
Ramon Garcia-Rojo
Ferenc Kun
Fréderic Lacombe
Reza Mahmoodi
Hans J. Tillemanns
Martin Wackenhut

Institute of Computational Physics, ICP,
University of Stuttgart, Germany

Seminario
Universitá Federico II,
Napoli, 19.XI.2004

Shear bands in granite of Pyrenees

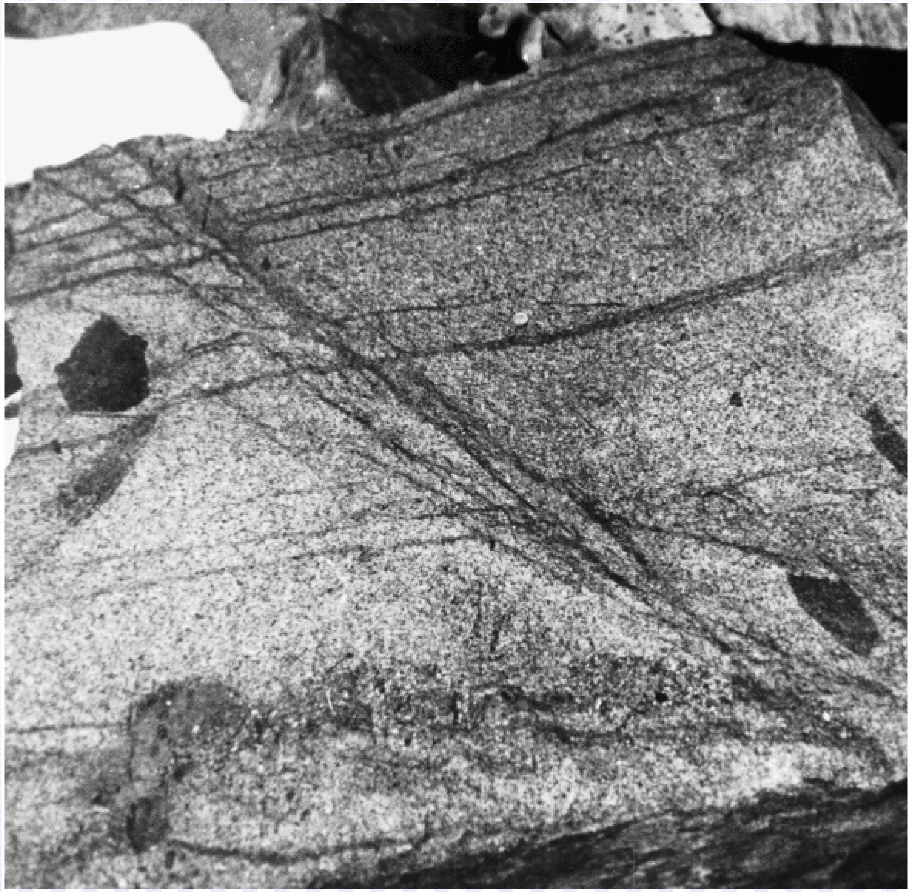

Starting configuration

- Imposed shear velocity
- Periodic boundary conditions
- Regularized polygons

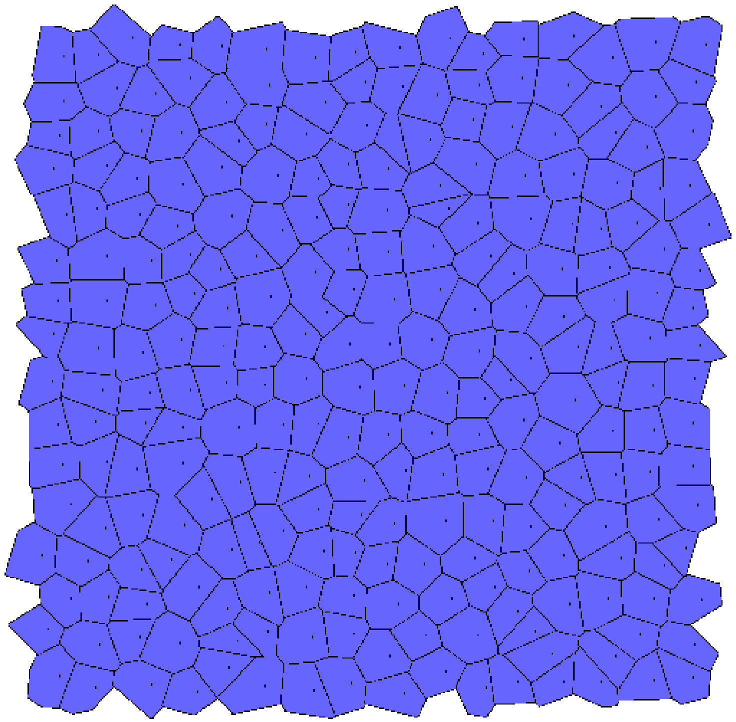

Molecular Dynamics for rigid polygons

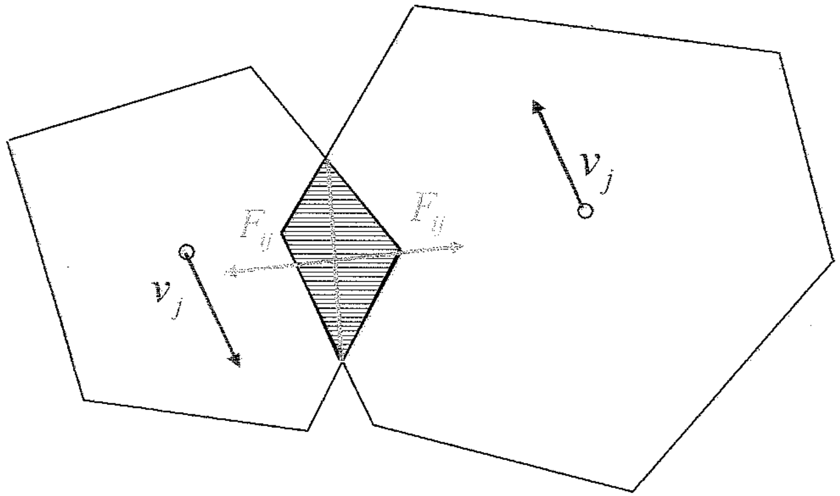

$$F_i = \sum_j F_{ij} + m_i g \qquad T_i = \sum_j T_{ij}$$

$$x_i(t+1) = x_i(t) + v_i(t)\Delta t$$

$$v_i(t+1) = v_i(t) + \frac{F_i}{m_i}\Delta t$$

$$\vdots$$

$$\varphi_i(t+1) = \varphi_i(t) + \omega_i(t)\Delta t$$

$$\omega_i(t+1) = \omega_i(t) + \frac{T_i}{I_i}\Delta t$$

$$\mathbf{F} = (YA/l)\,\mathbf{n} - \gamma v^{(n)}\,\mathbf{n} - min(\gamma v^{(t)}, \mu F^{(n)})\,\mathbf{t}$$

Force distribution in a polygonal packing

Contact forces

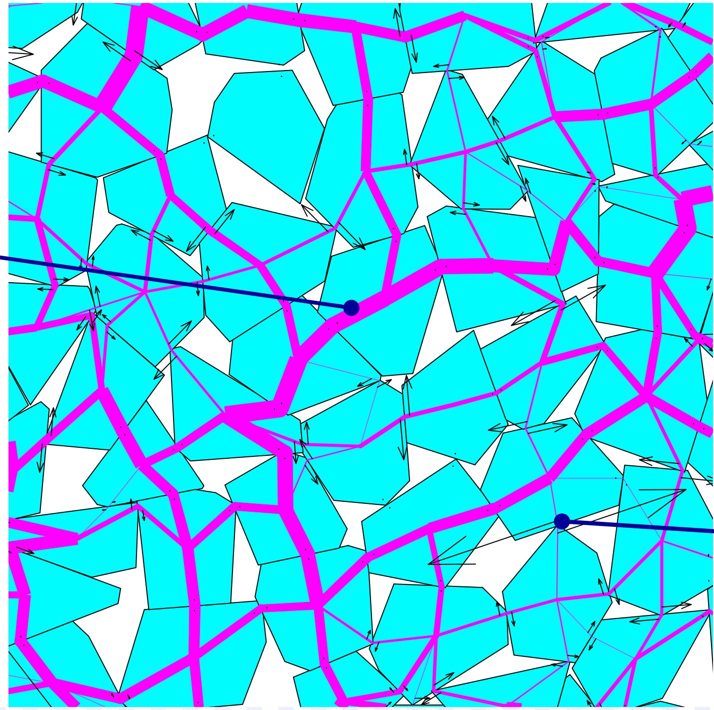

Contact displacements

Kinetic energy after displacement

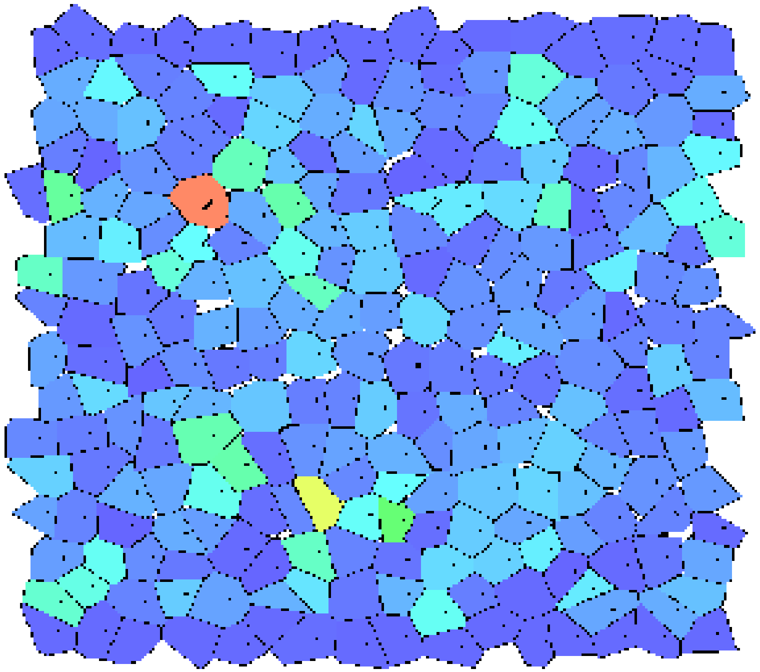

- Blue: Low energy
- Red: High energy

Grains with more than three degrees rotation

Localized shear band

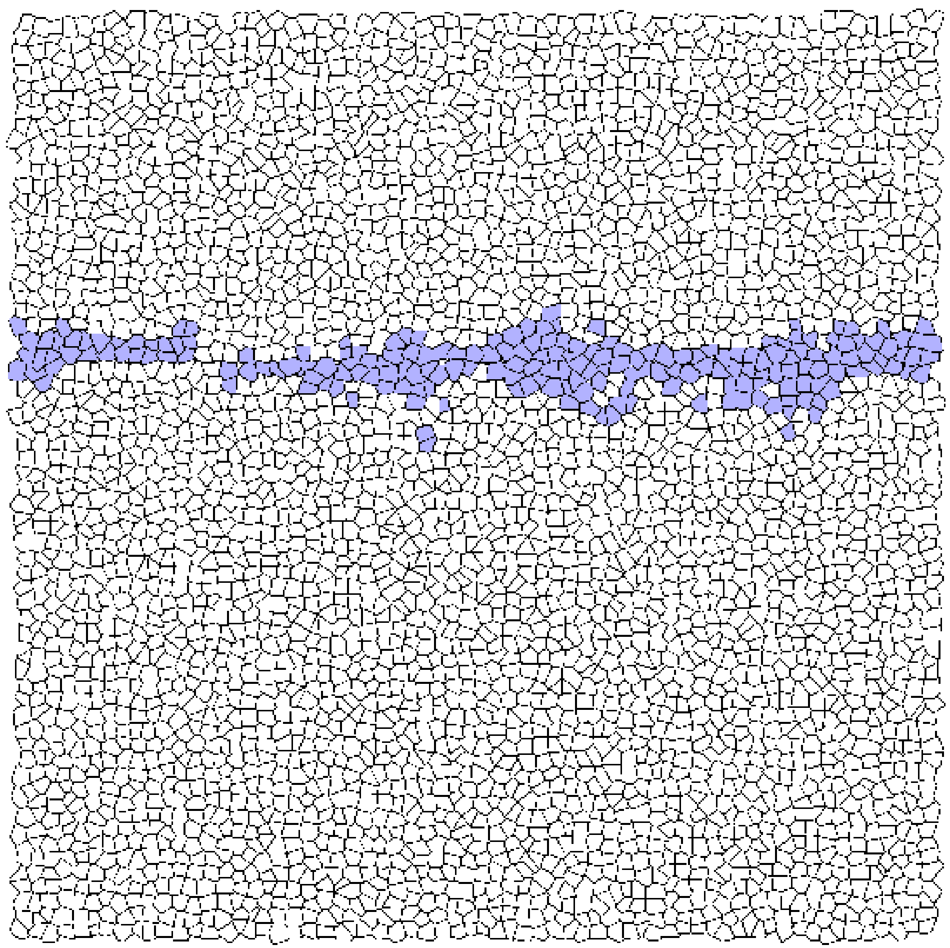

Shear forces

Dependence on time, velocity, and normal force.

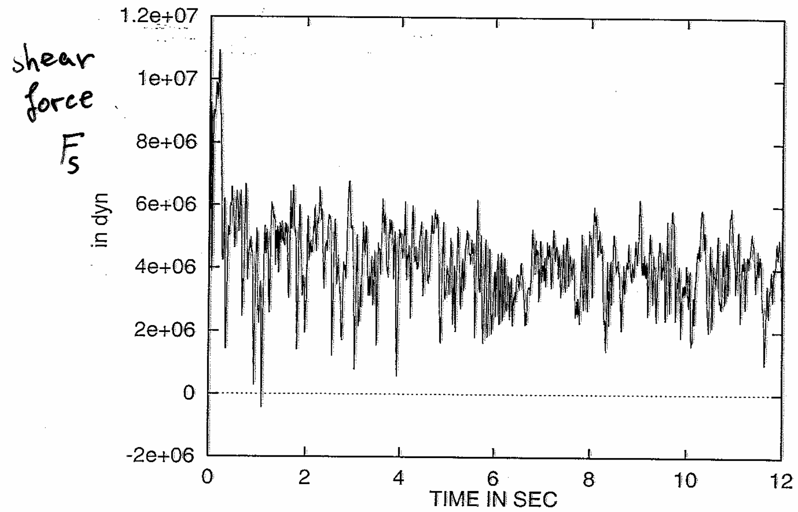

shear hardening $F_s \sim v_s^{1/6} F_n^{3/4}$

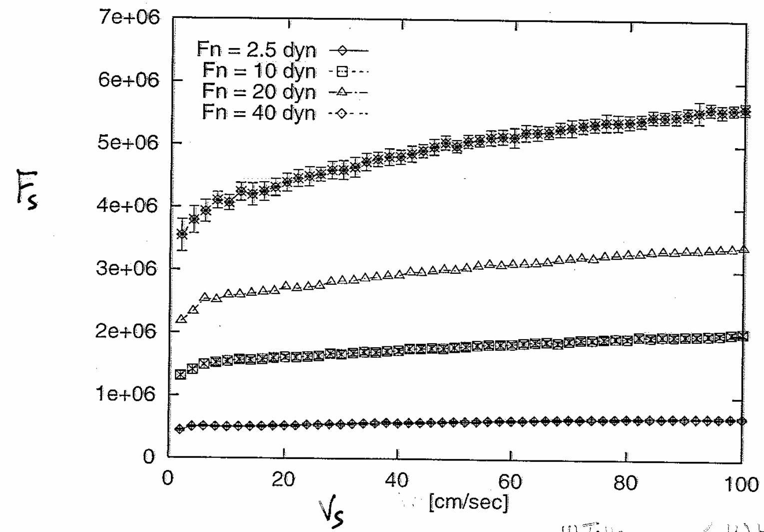

Shear force in dyn versus shear velocity in cm/s for four different normal forces.

H.J. Tillemans & H.J. Herrmann

Dilatancy

Dependency on velocity,
and normal force.

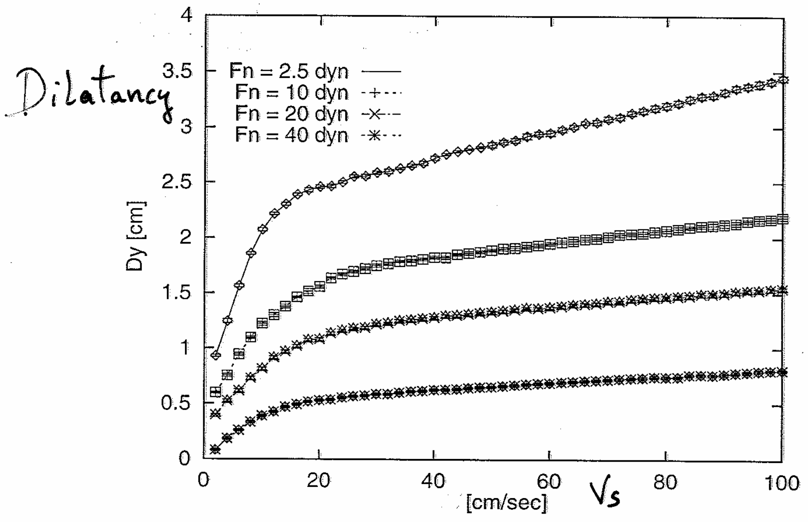

Dilatancy in cm versus shear velocity in cm/s for four different normal forces .

$$\frac{dy}{dV_s} \propto \frac{1}{\sqrt{F_n}}$$

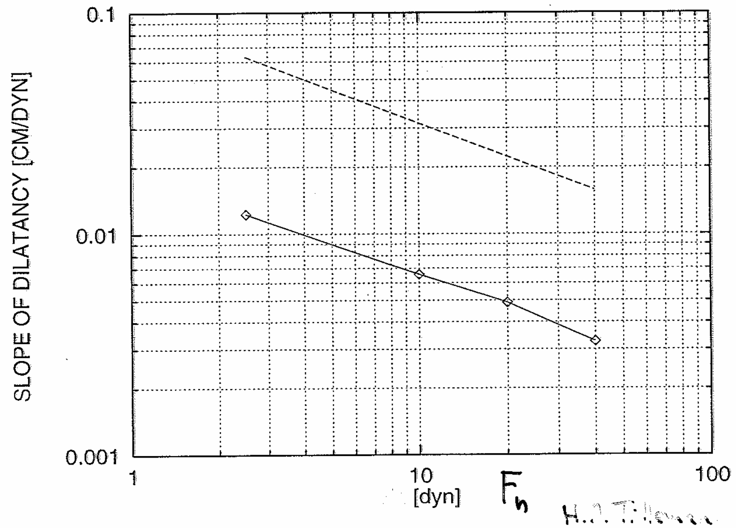

Kinetic energies

- Bursts.
- Gutenberg-Richter law.

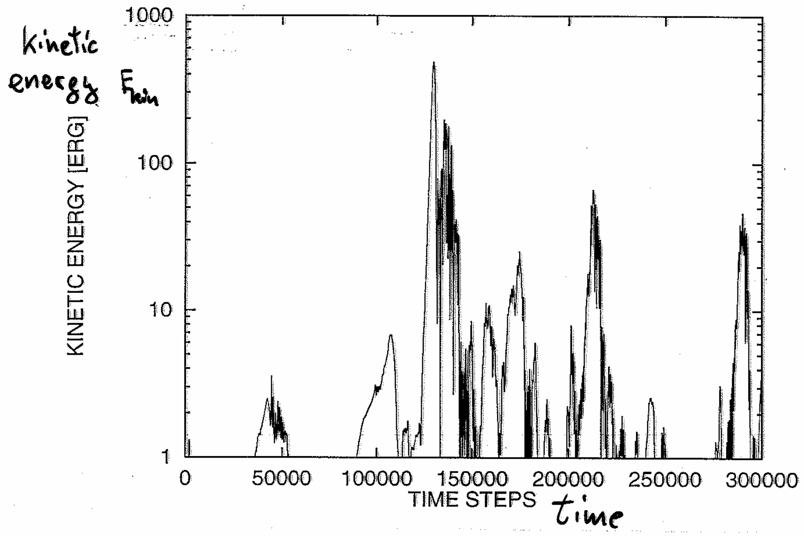

Gutenberg-Richter law

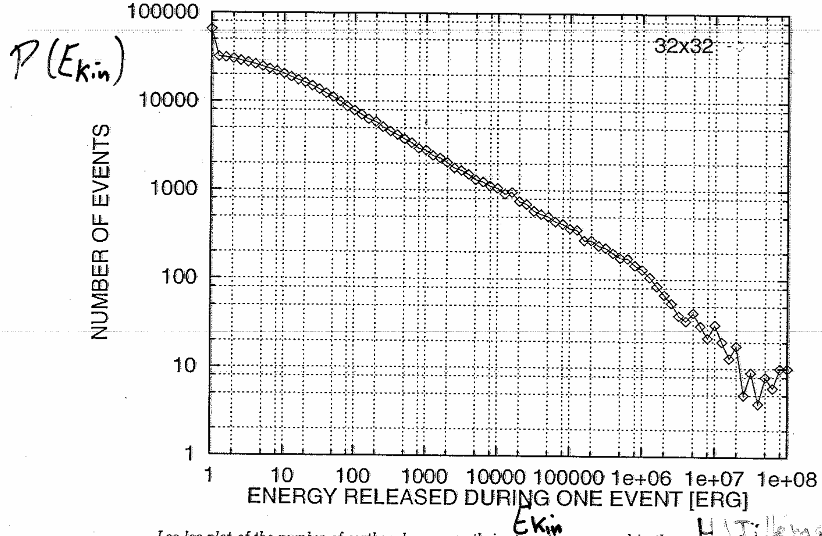

Log-log plot of the number of earthquakes versus their strengths measured in the energy released during one event. The slope of the curve obtained by a logarithmical binning is 0.4

Two-dimensional Couette cell

Experiment

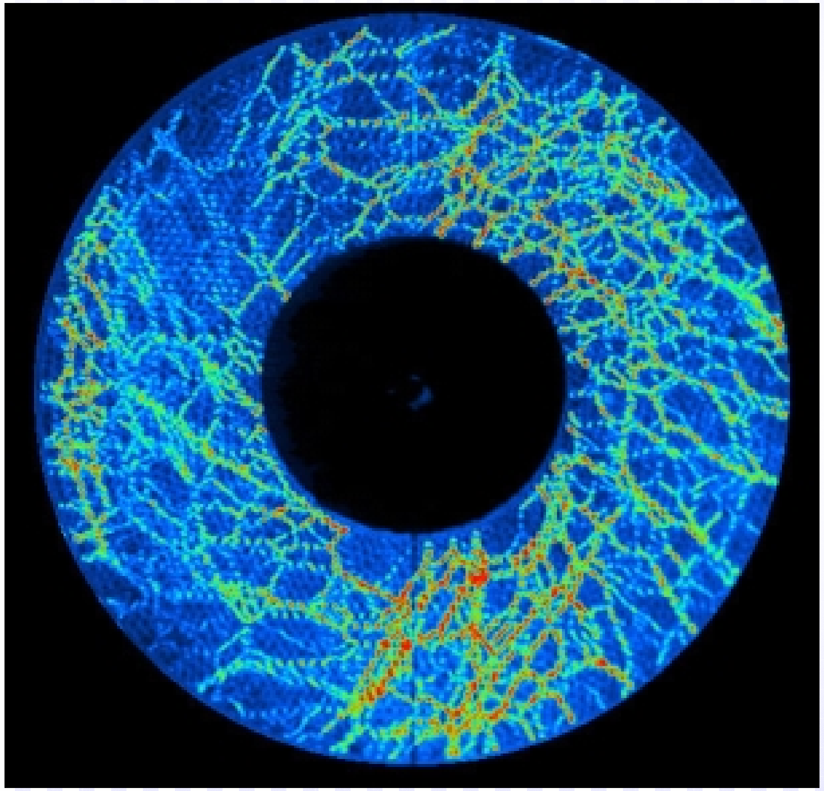

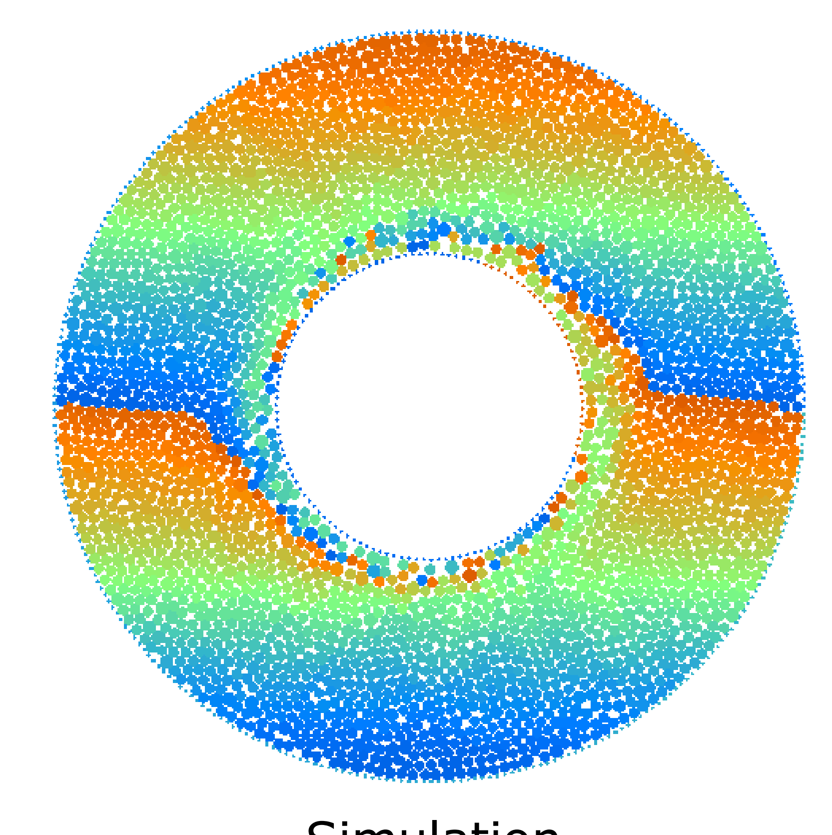

Simulation

Two-dimensional Couette cell

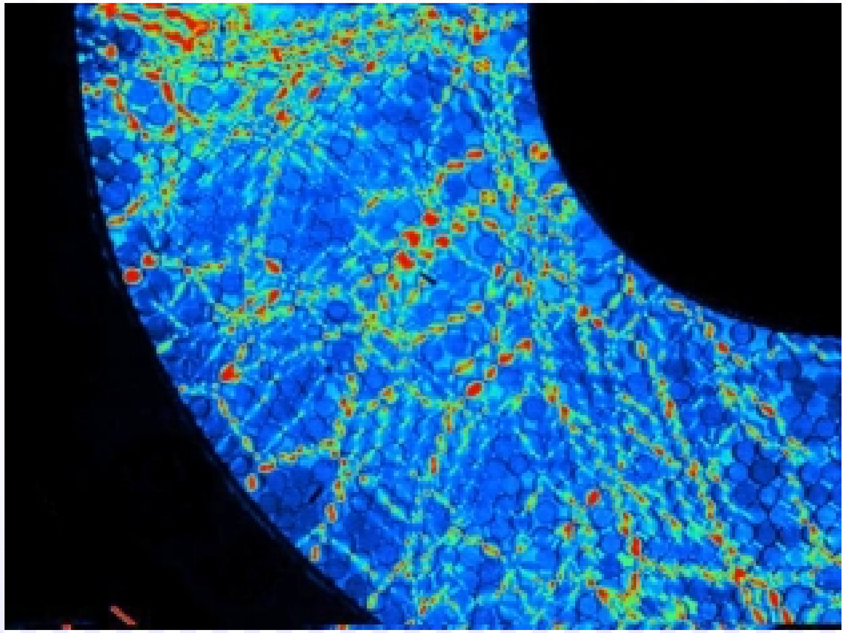

Close-up

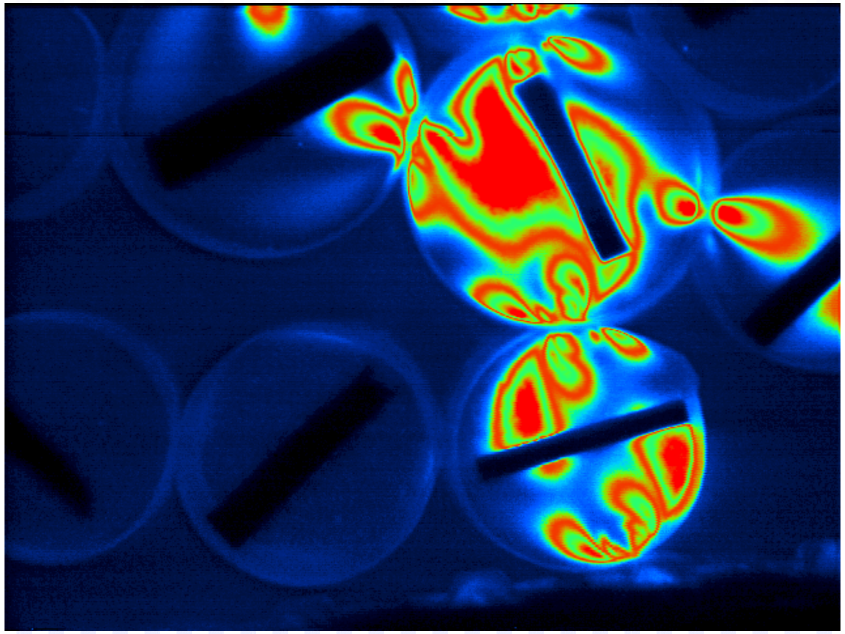

Mean tangential velocity and spin

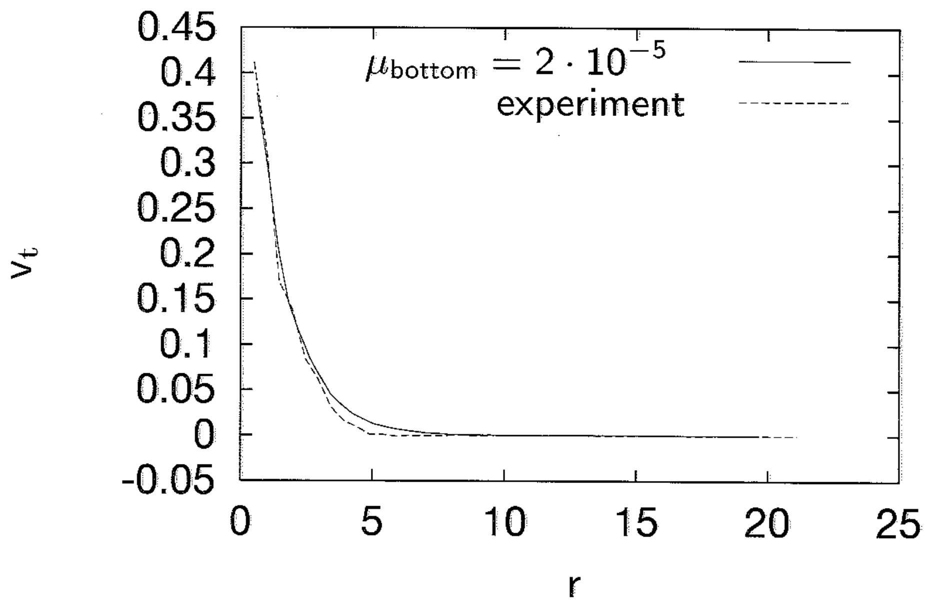

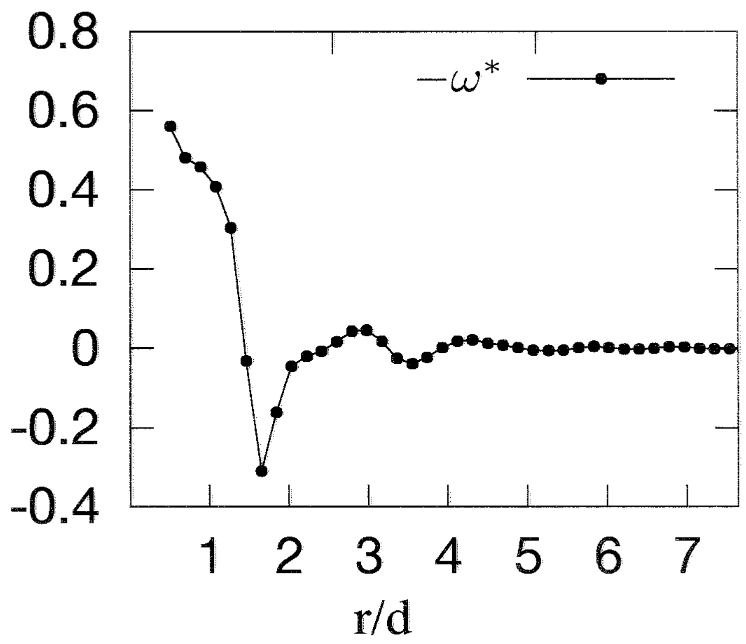

Comparison of experiments and simulation

Spin Distribution

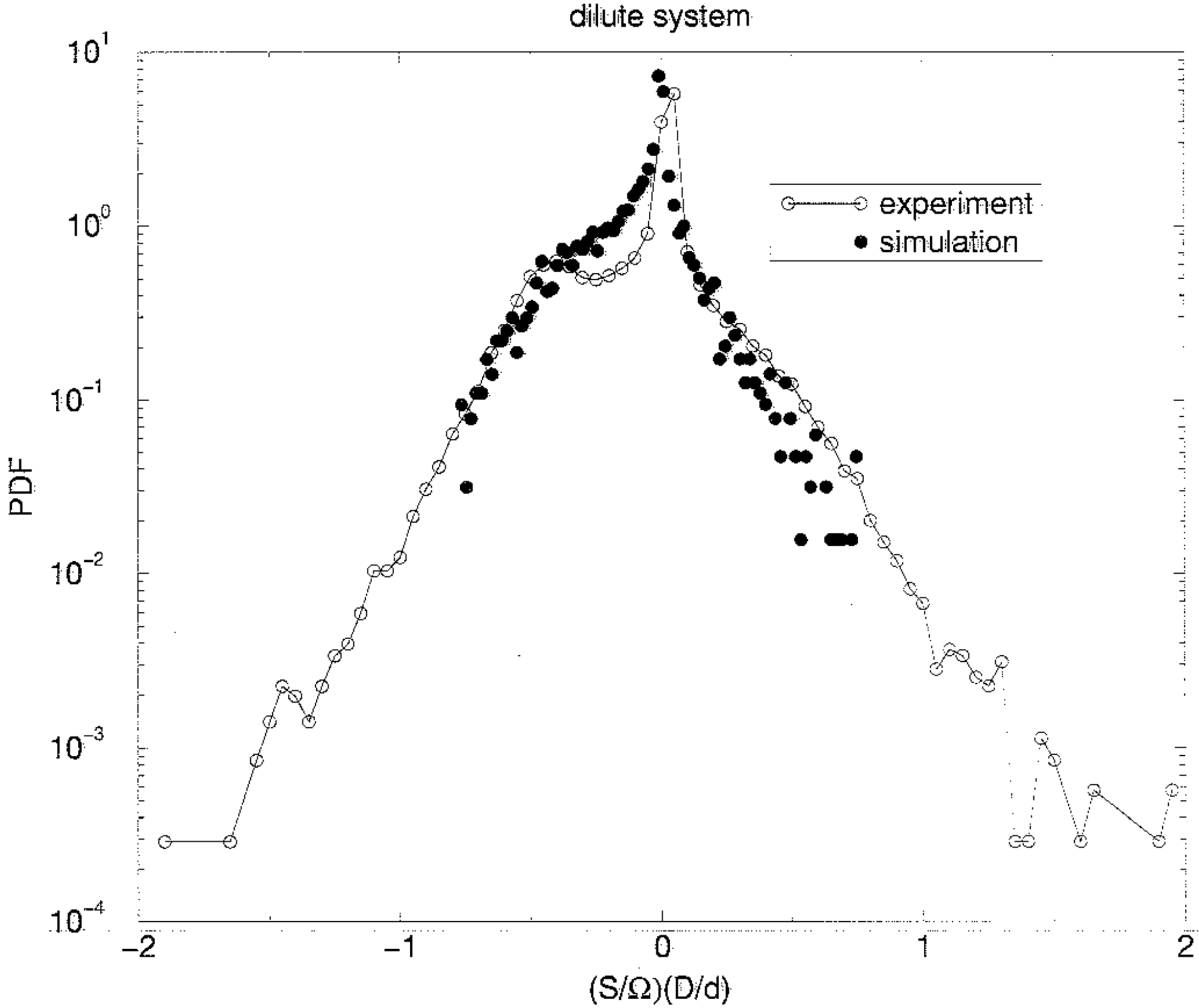

probability of contact angles

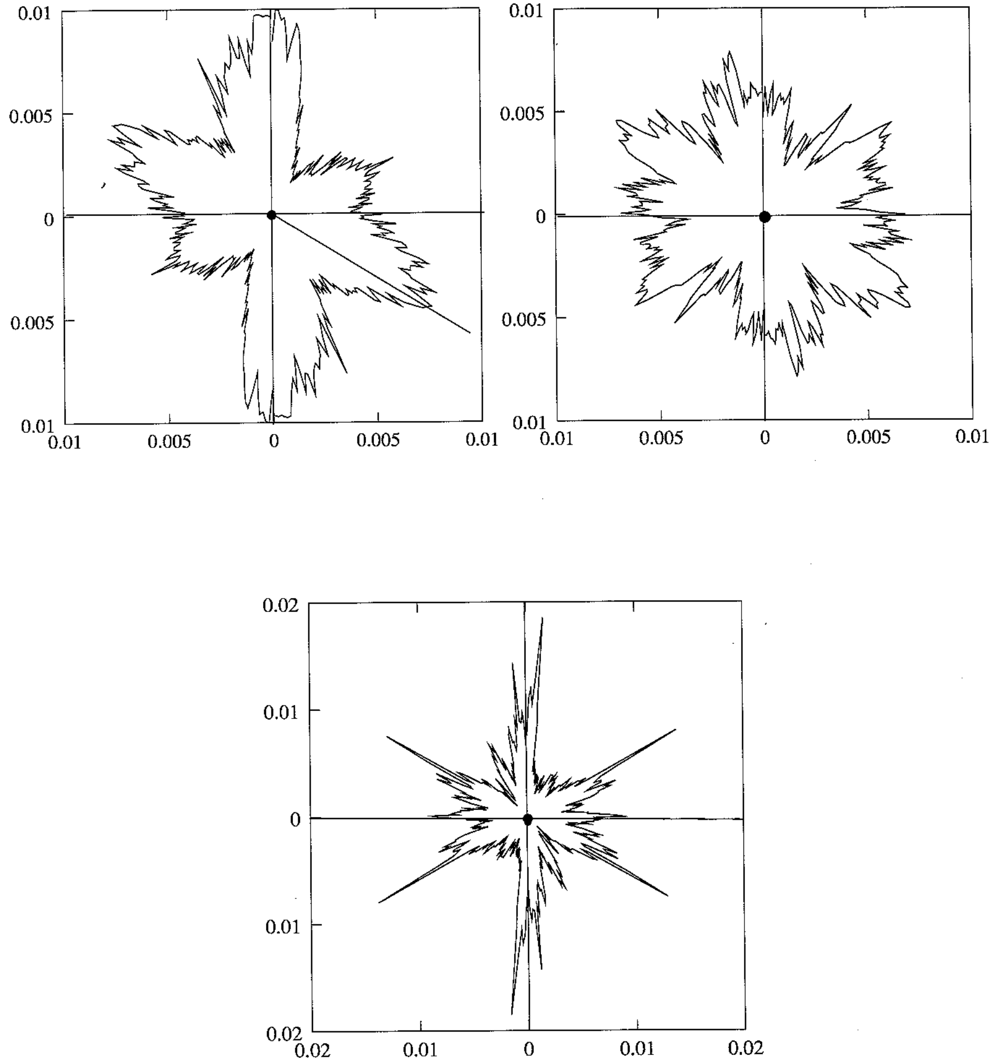

Polar distribution at different positions:

- Inside shear band
- At boundary
- Outside

Uniaxial compression

- If the confining pressure is above a certain threshold, a continuous localization of the deformation comes up as the stress increases.

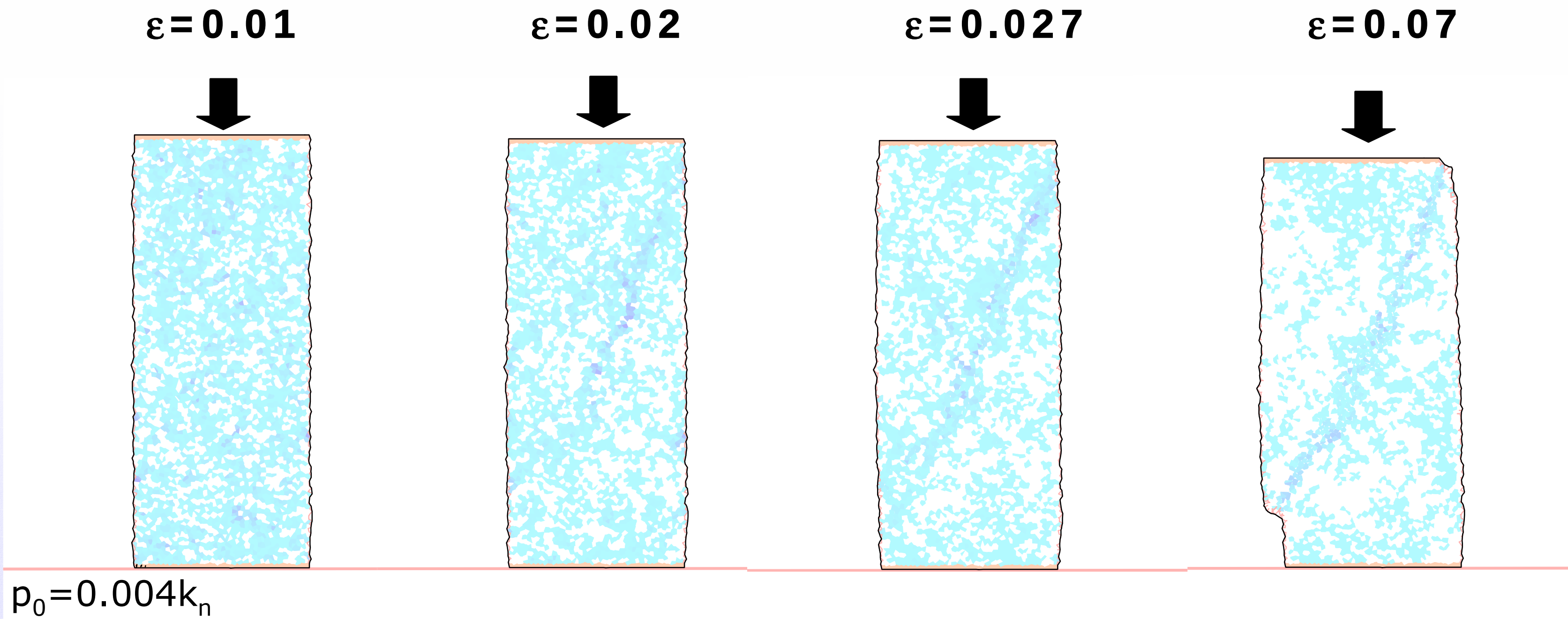

Biaxial test boundary conditions
Membrane:Floppy boundary

- The smallest convex polygon enclosing the boundaries is chosen. Its lowest point is the first vertex of the perimeter.
- The boundary points are iteratively included using the bending criterion. (Θ_{th} is the threshold angle for bending)
- The final result gives a set of segments lying on the boundary of the sample.

$\Theta_{th} = \pi$ | $\Theta_{th} = 3\pi/4$ | $\Theta_{th} = \pi/2$ | $\Theta_{th}=\pi/4$

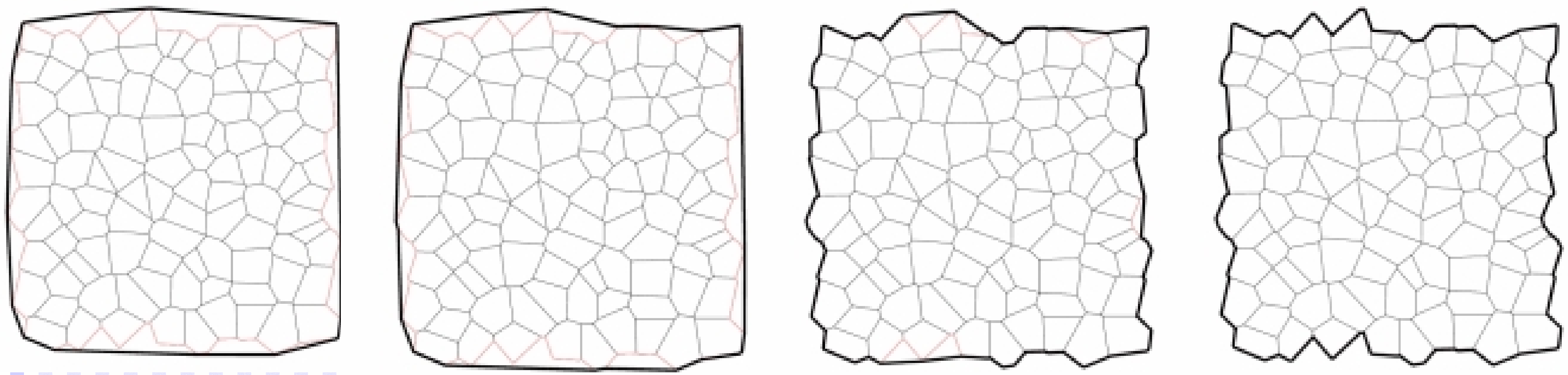

Biaxial test boundary conditions
Force on the membrane

- On each segment of the membrane:

$$\vec{T} = \Delta x_1 \hat{x}_1 + \Delta x_3 \hat{x}_3,$$

- We apply the force:

$$\vec{f}^m = -\sigma_1 \Delta x_3 \hat{x}_1 + \sigma_3 \Delta x_1 \hat{x}_3 - \gamma_b m_i \vec{v}^i$$

- One must take into account whether the segment of the membrane fully coincides with a polygon wedge, or whether it connects the vertices of two polygons.

Biaxial test

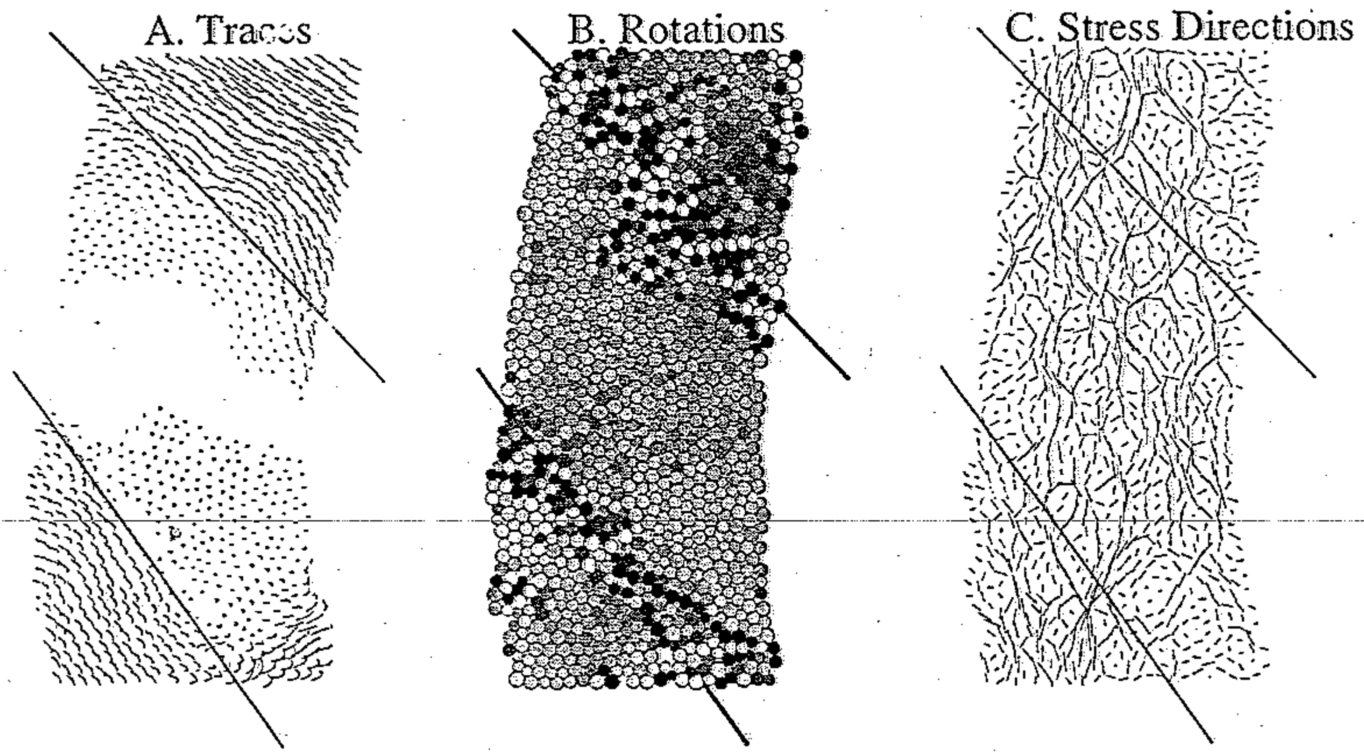

Spontaneous bearing formation

Black: clockwise rotation

White: counter-clockwise rotation

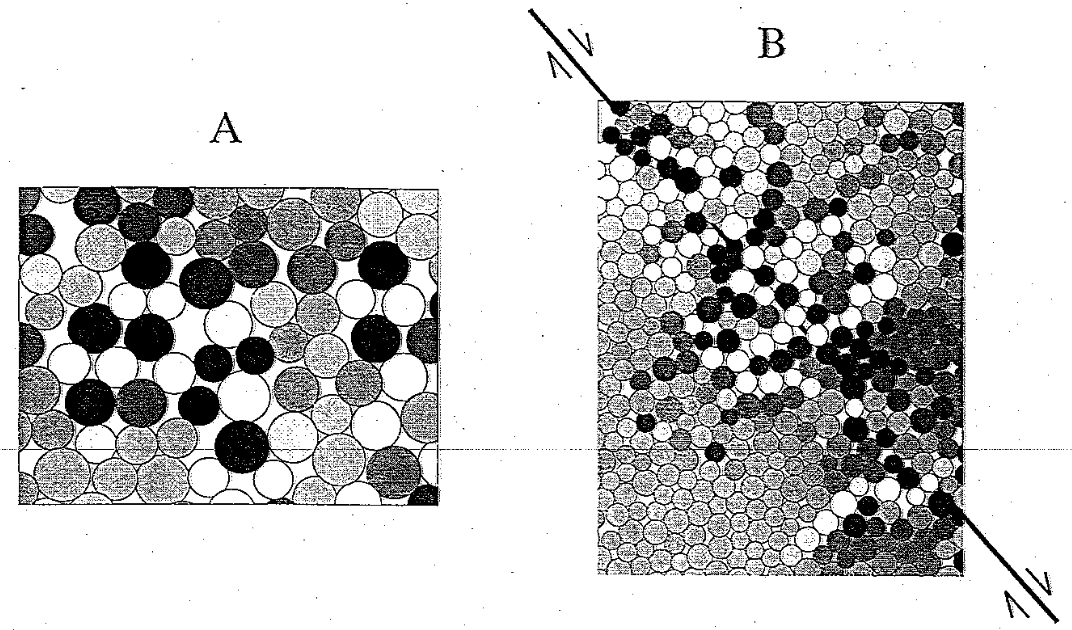

Close-up of bearing

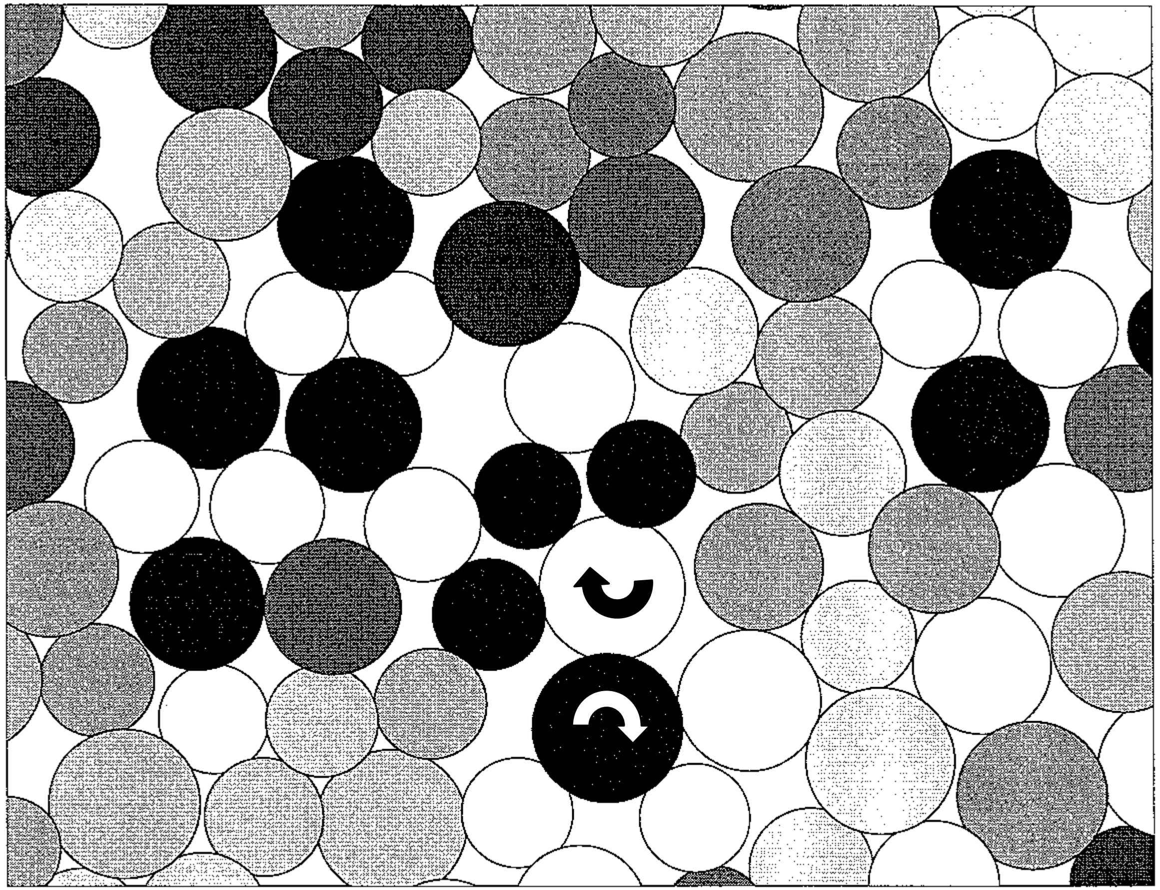

Rotations in the system

Incremental particle displacement after one cycle

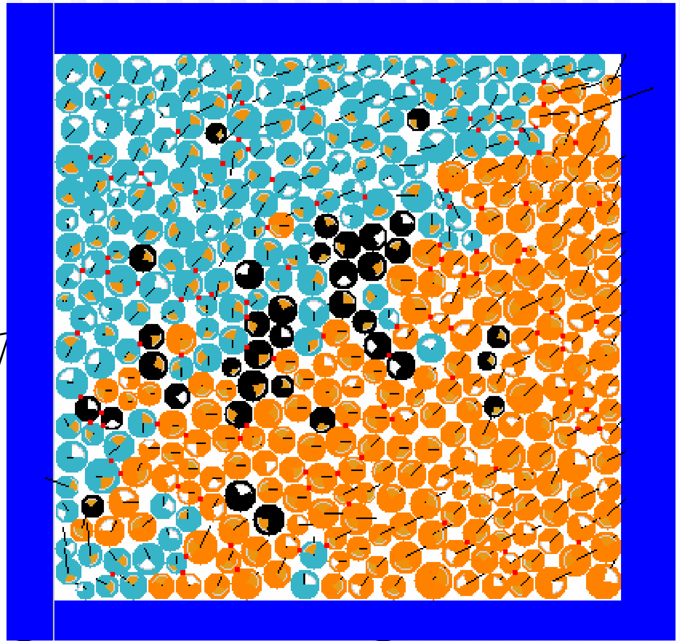

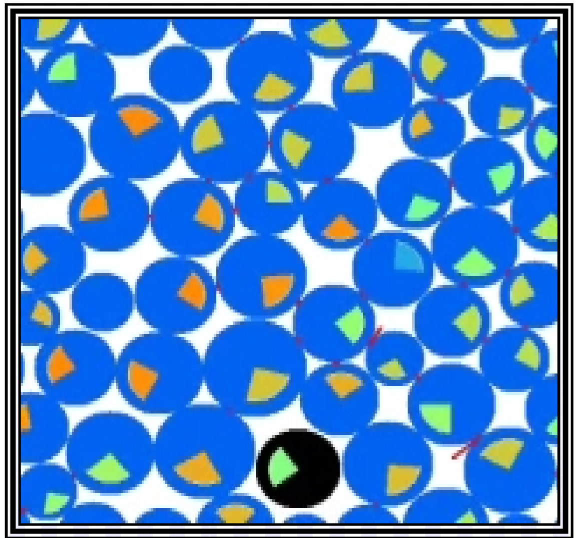

Rotation and sliding during cyclic loading

Idealized space filling bearing

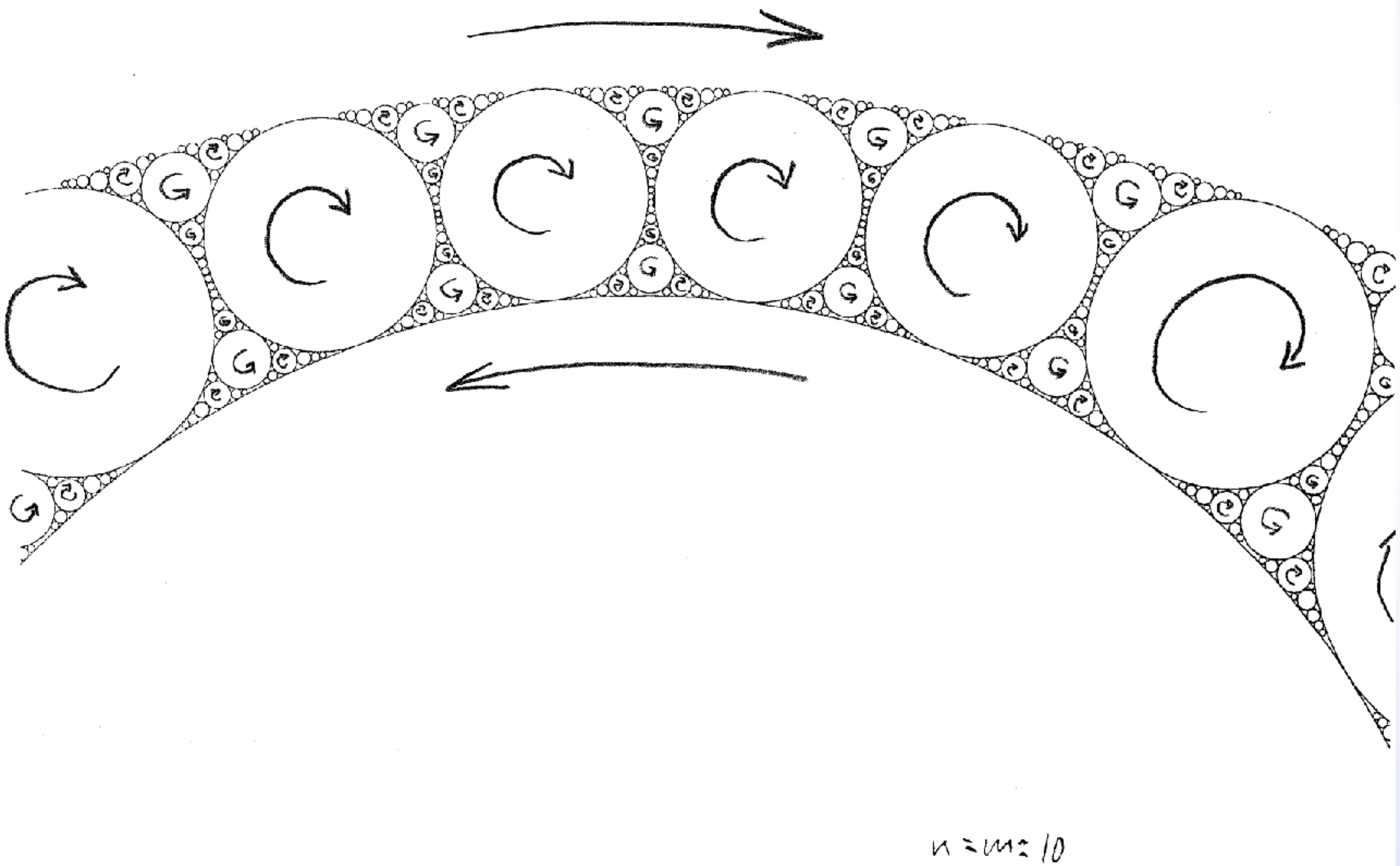

Example for space filling bearing

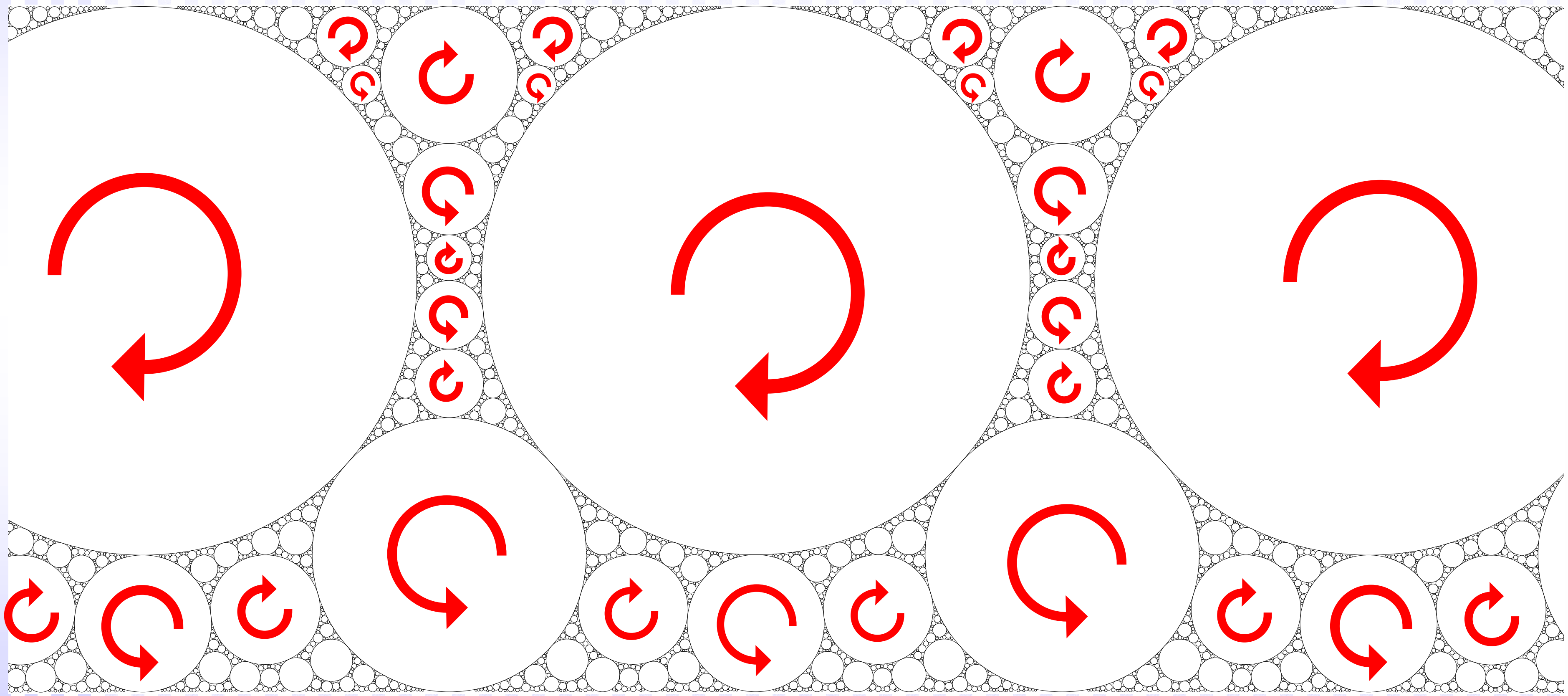

Random bearing

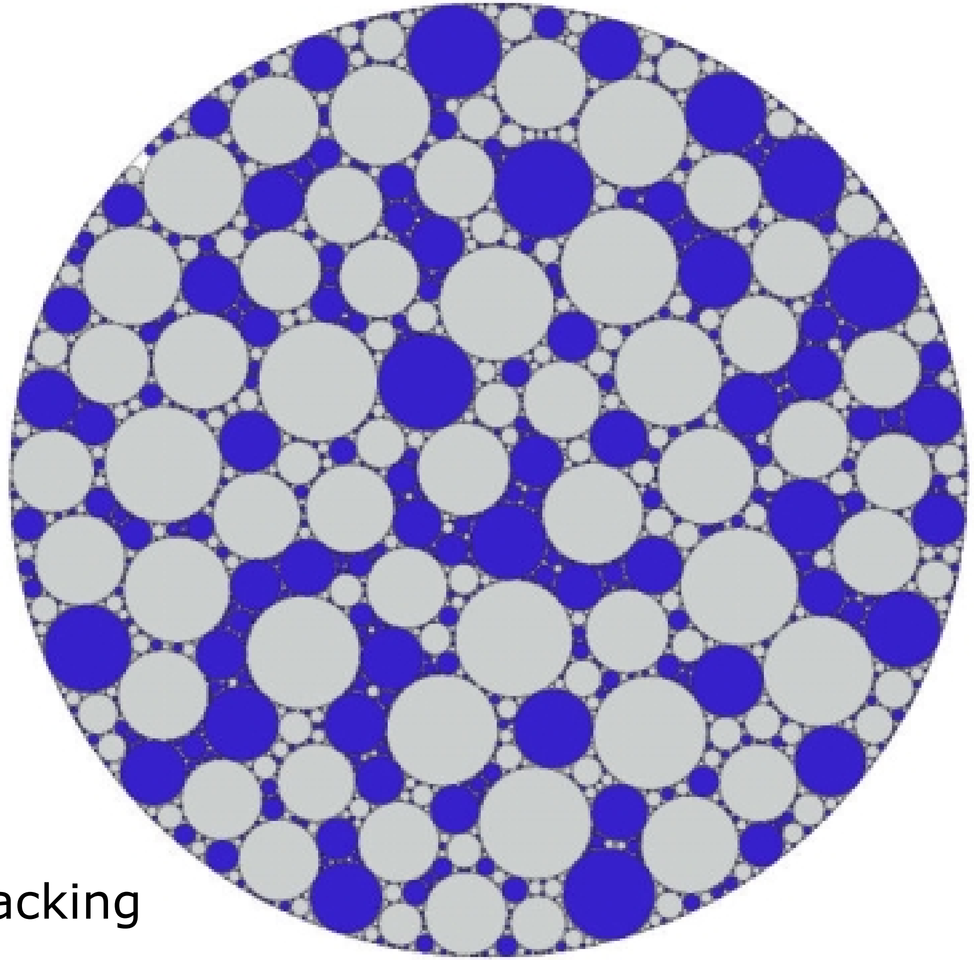

Bi-chromatic packing

Rolling space-filling bearings

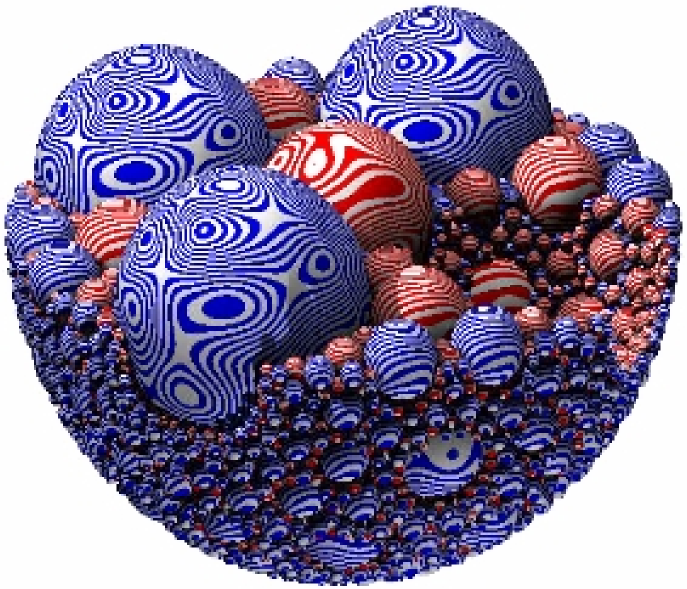

$c = 0.0$

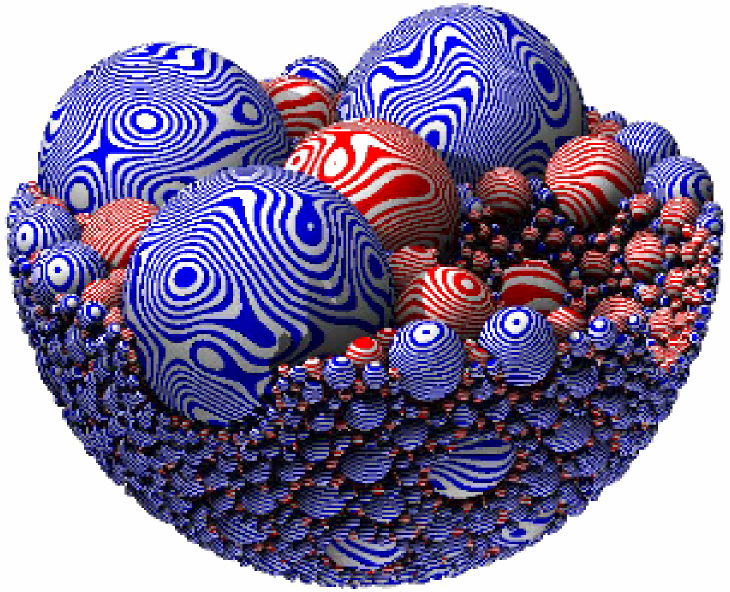

$c = 0.5$

Granular ratcheting

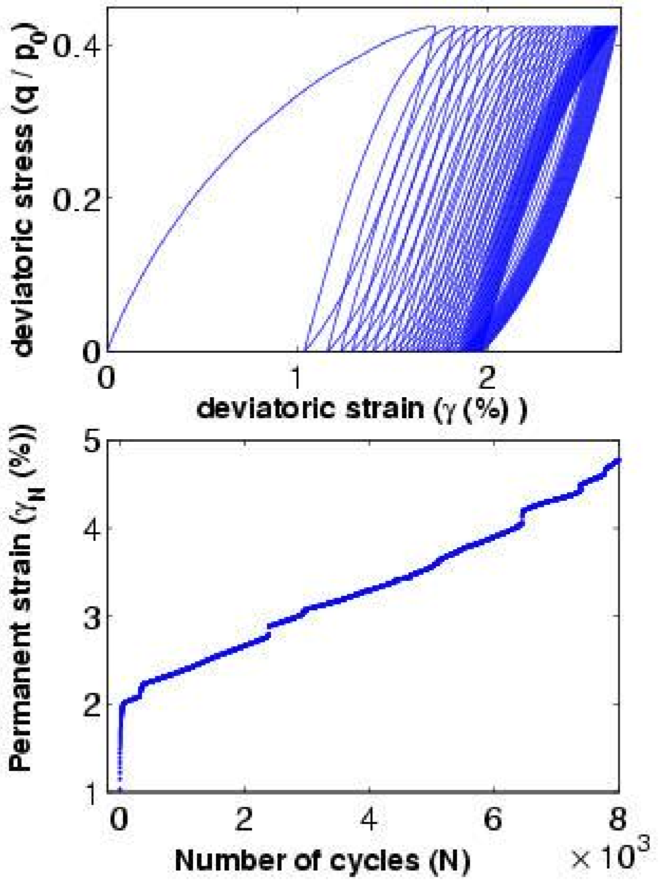

Cyclic uniaxial loading

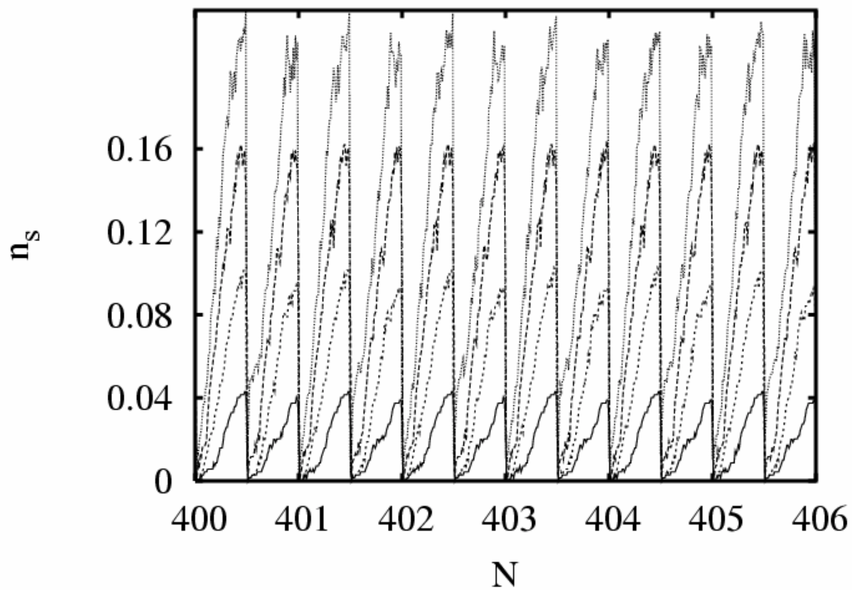

Vorticity in ratcheting

Displacement field

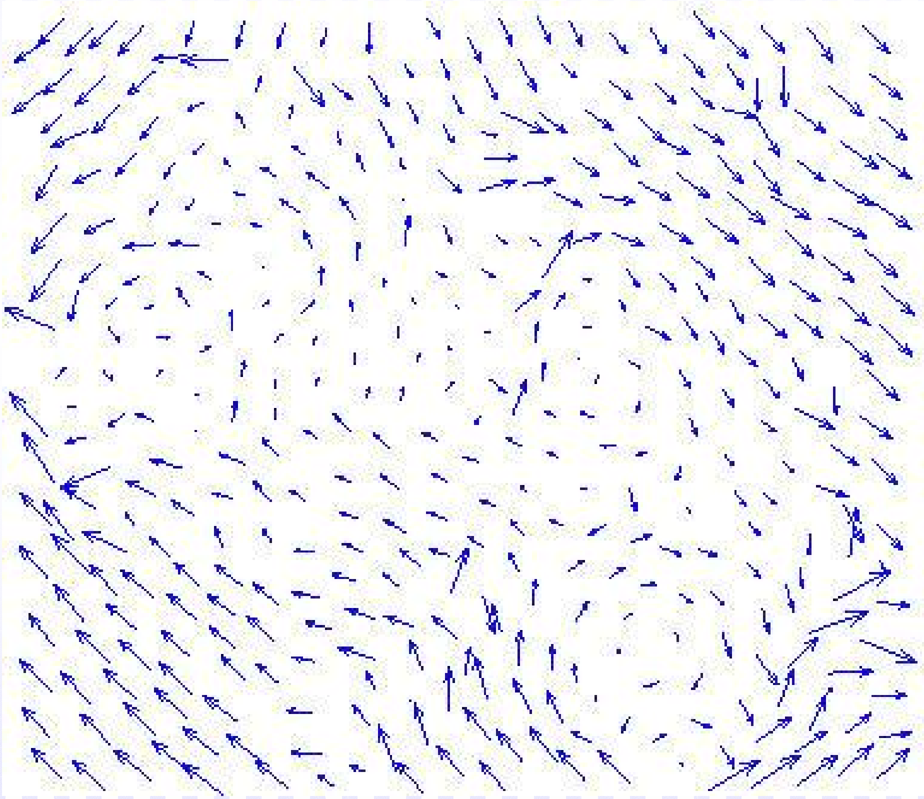

Characterization of the granular ratcheting

- Strain rate and the resilient parameters characterize the ratcheting regime.

$$M_R = \frac{\Delta\sigma}{\gamma_R}.$$

$$\zeta = -\frac{\epsilon_1^R}{\epsilon_2^R}.$$

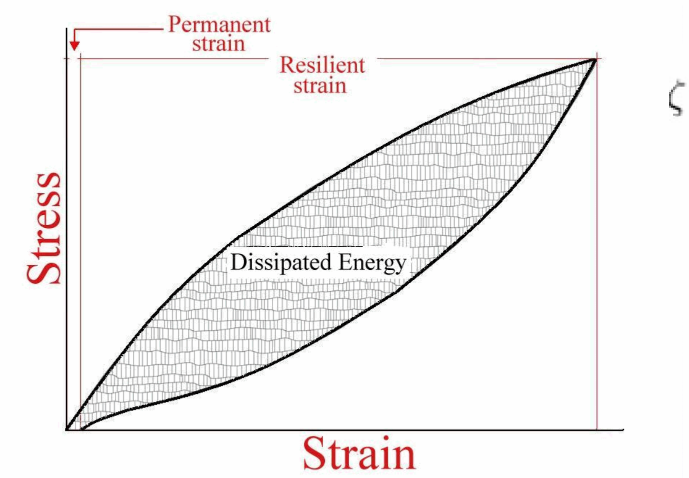

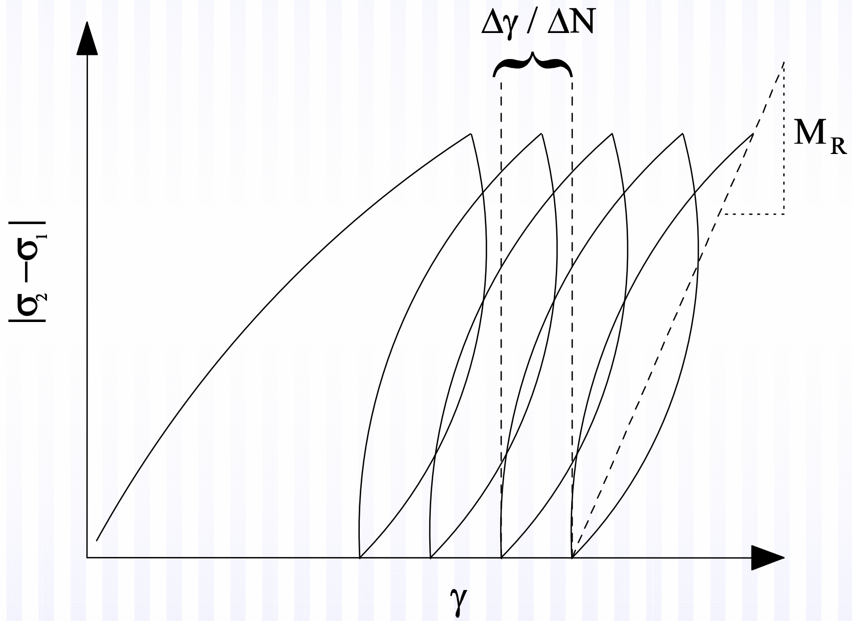

- The effect on these magnitudes of the macroscopic (confining pressure, deviator) and microscopic quantities (stiffness, friction) can be investigated with our model.

Contact forces and plastic deformation

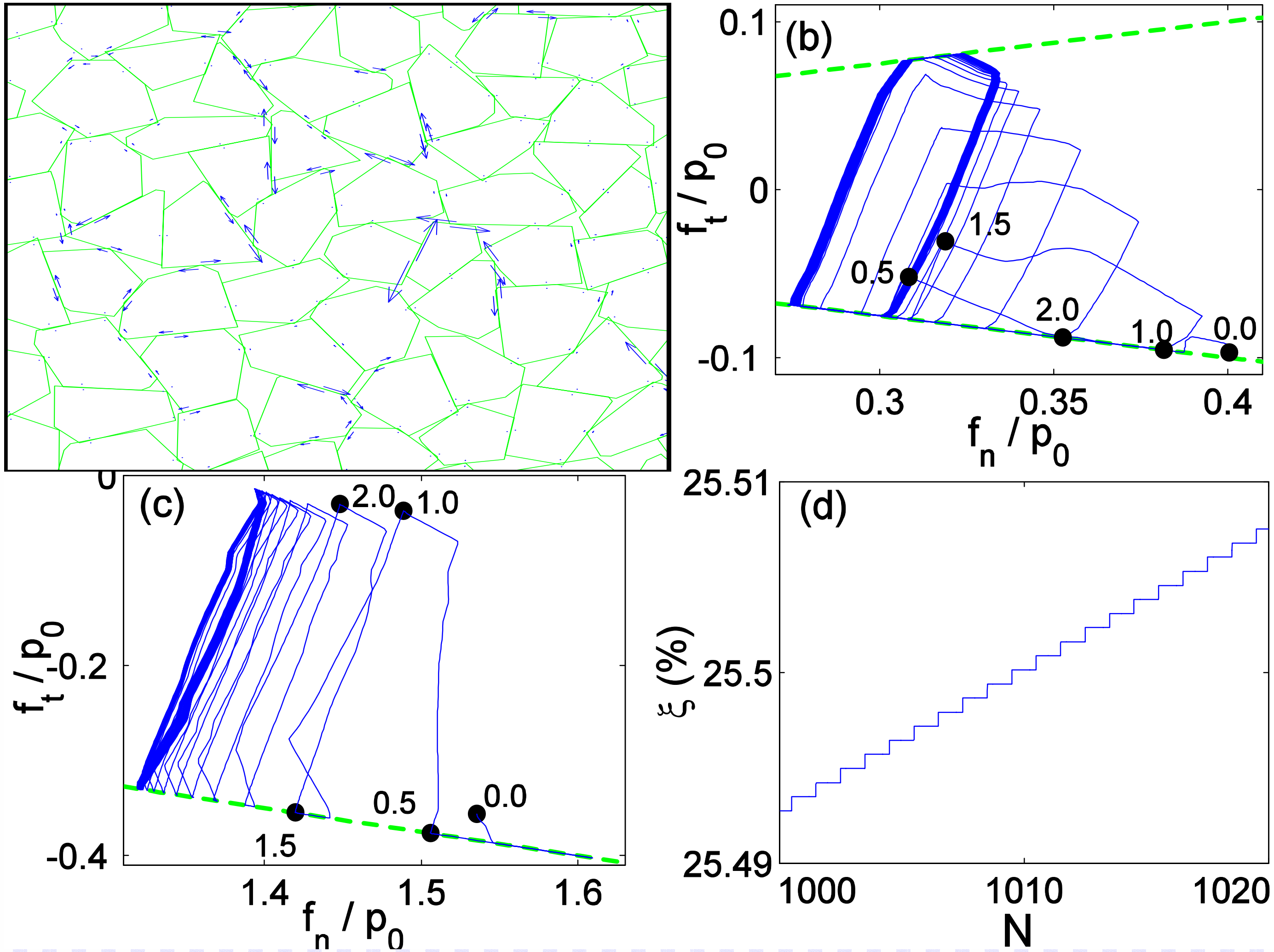

Permanent strain accumulation

- Power law dependence on the confining pressure and the deviatoric stress.

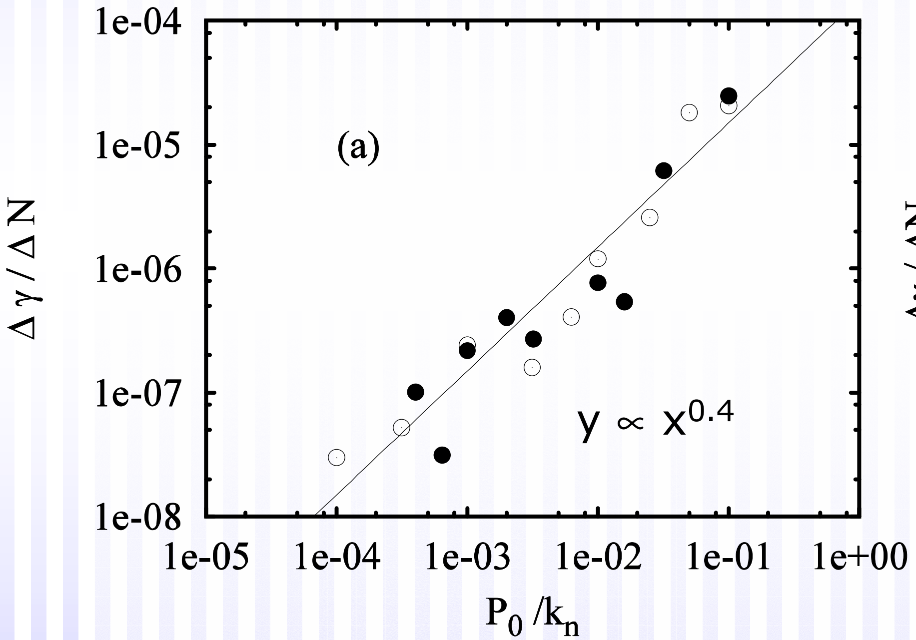

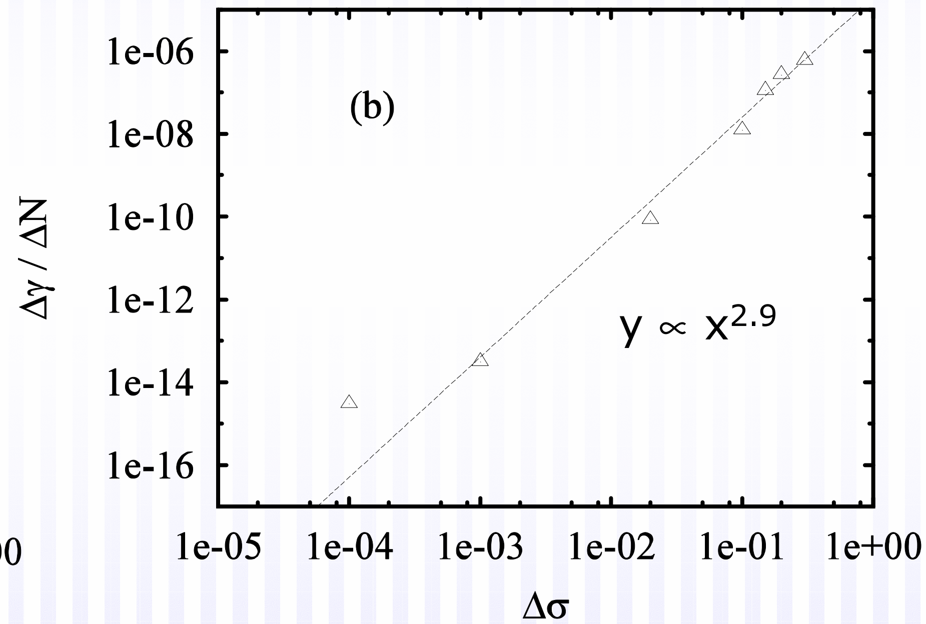

P_0 confining pressure

$\Delta\sigma$ loading amplitude

Permanent strain accumulation

k_t tangential grain stiffness
k_n normal grain stiffness

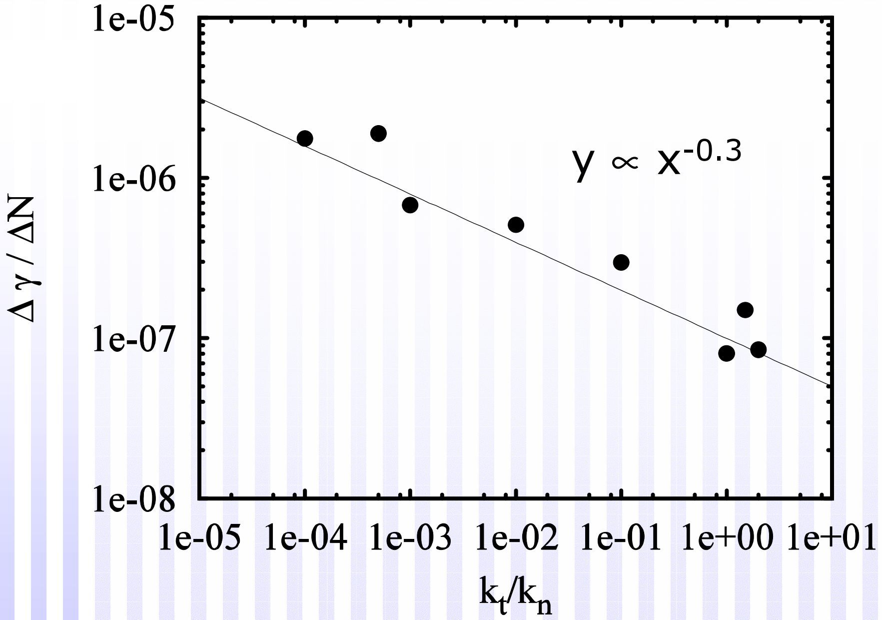

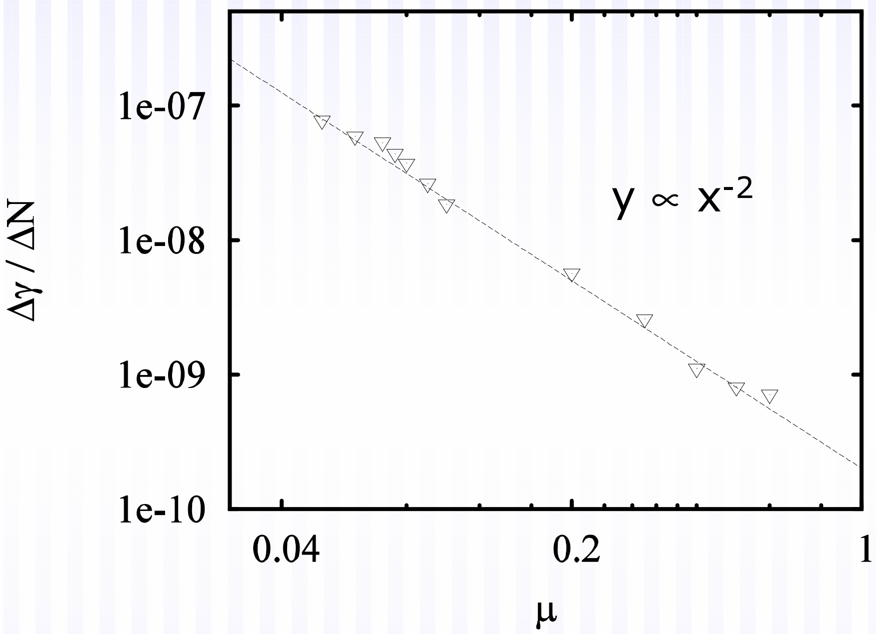

μ, friction coefficient

Resilient response

- Close to the shakedown limit, the resilient parameters remain approximately constant.

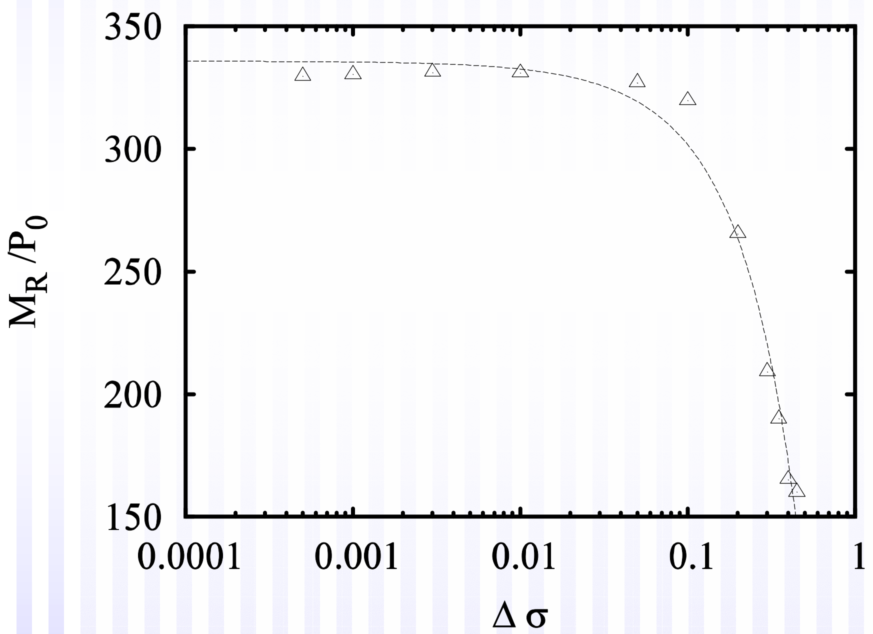

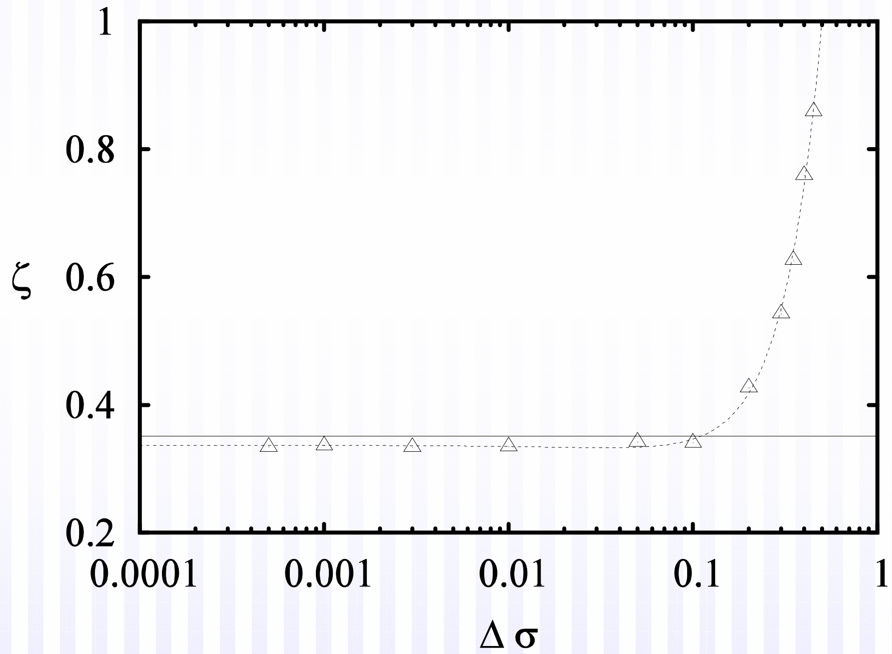

- For higher $\Delta\sigma$, a there is a polynomial dependence on $\Delta\sigma$ of both resilient magnitudes.

Resilient response

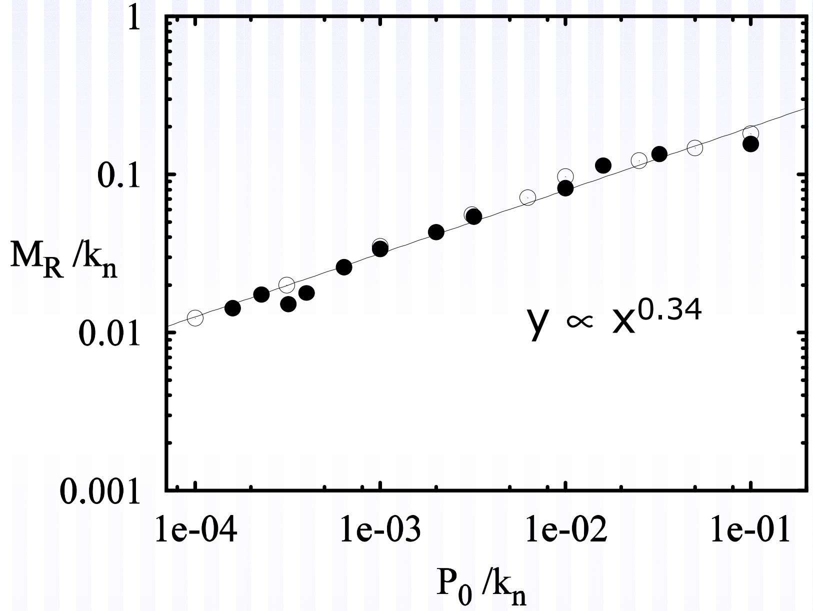

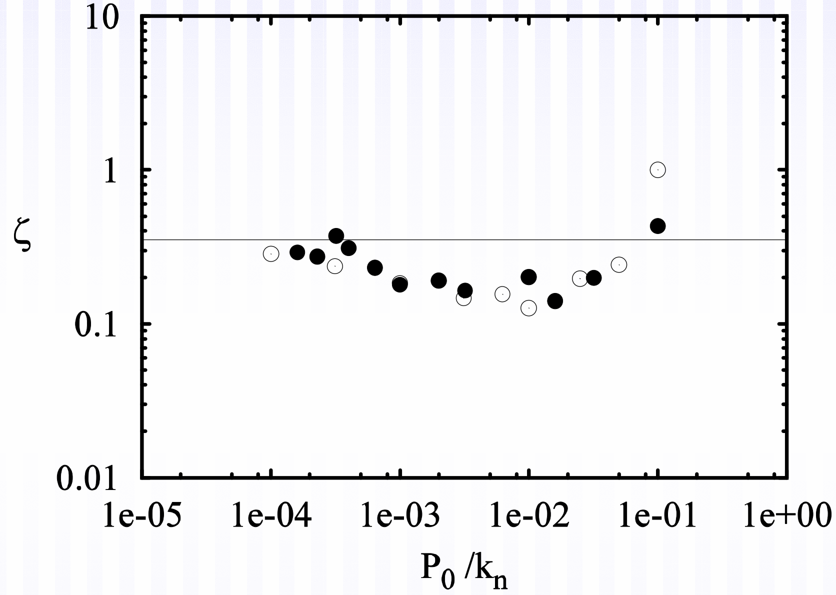

- $M_{R,}$ resilient modulus
- ζ, Poisson ratio

Shakedown

- Relaxation of the dissipated energy per cycle.

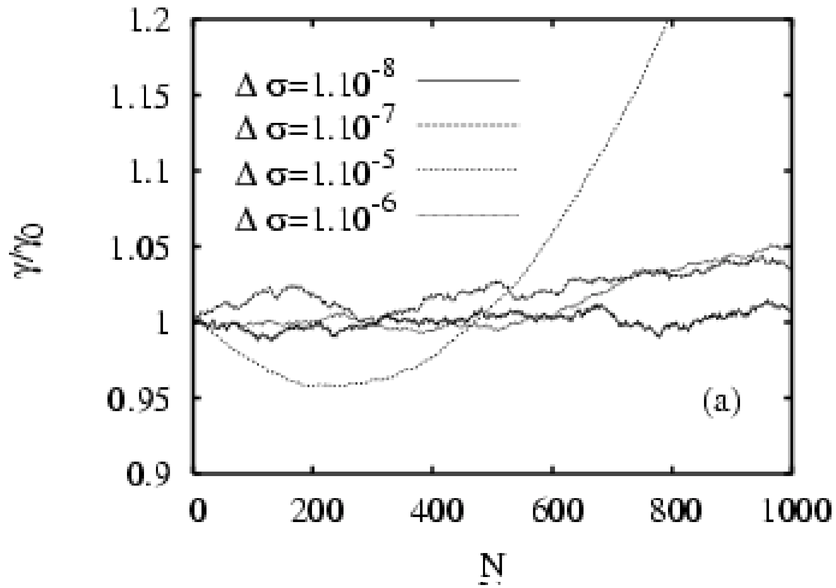

- Non-systematic accumulation of permanent strain.
- No sliding contacts.
- …all dissipation is due to the viscosity.

Drucker-Prager plasticity

- Mohr-Coulomb criterion

  $\tau = p \tan \varphi + C$
  φ = friction angle ($\varphi \approx 30°$)
  C = cohesion force

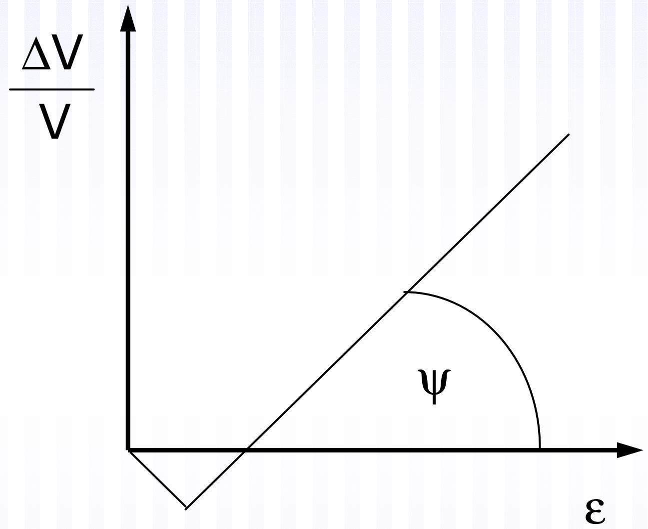

- Plastic flow rule

  ψ = dilation angle ($\psi \approx 11°$)
  non-associate $\varphi \neq \psi$

FLAC calculation of pure shear

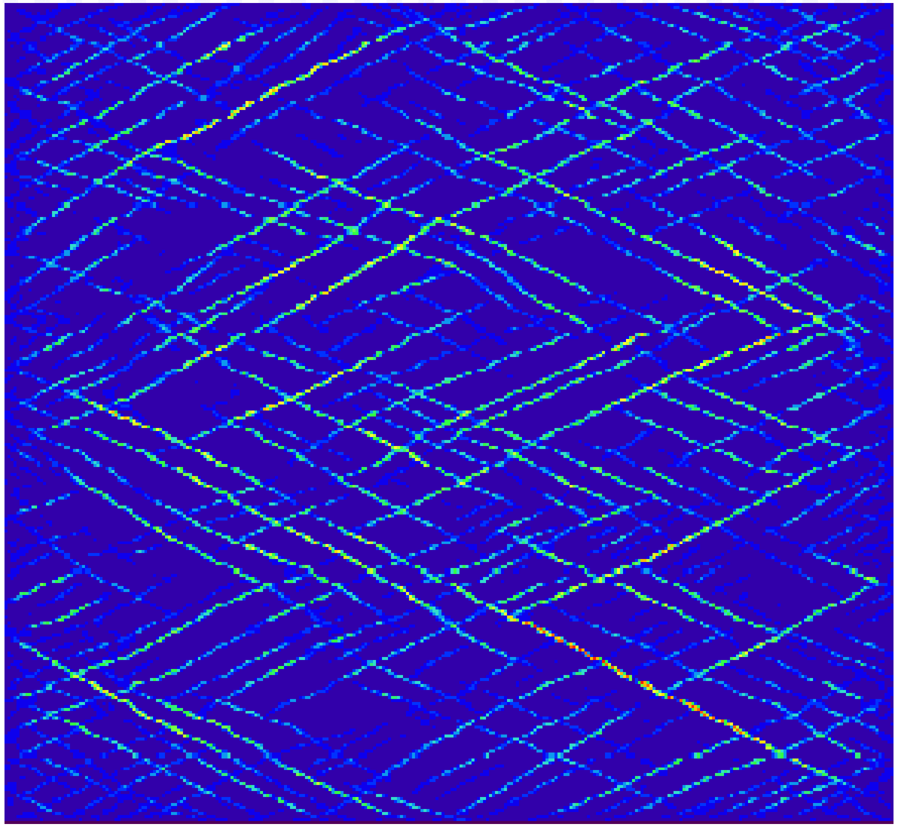

- Fractal network
- Mesh dependence

Statistical argument for finite width of shear band

On the width of shear bands

H J Herrmann

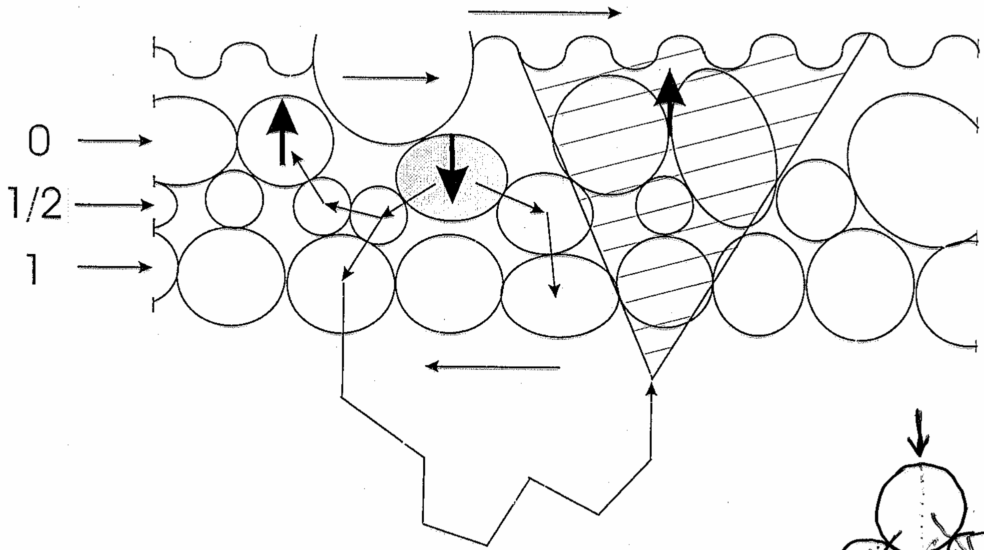

FIG. 1

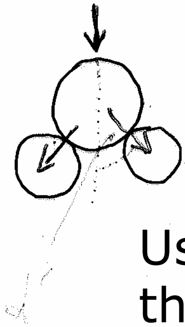

Using Martingales, one obtains the number of force chains that turn upwards giving an overage with of 15 grain diameters

Fragmentation in shear bands

Shear bands become denser and stiffer

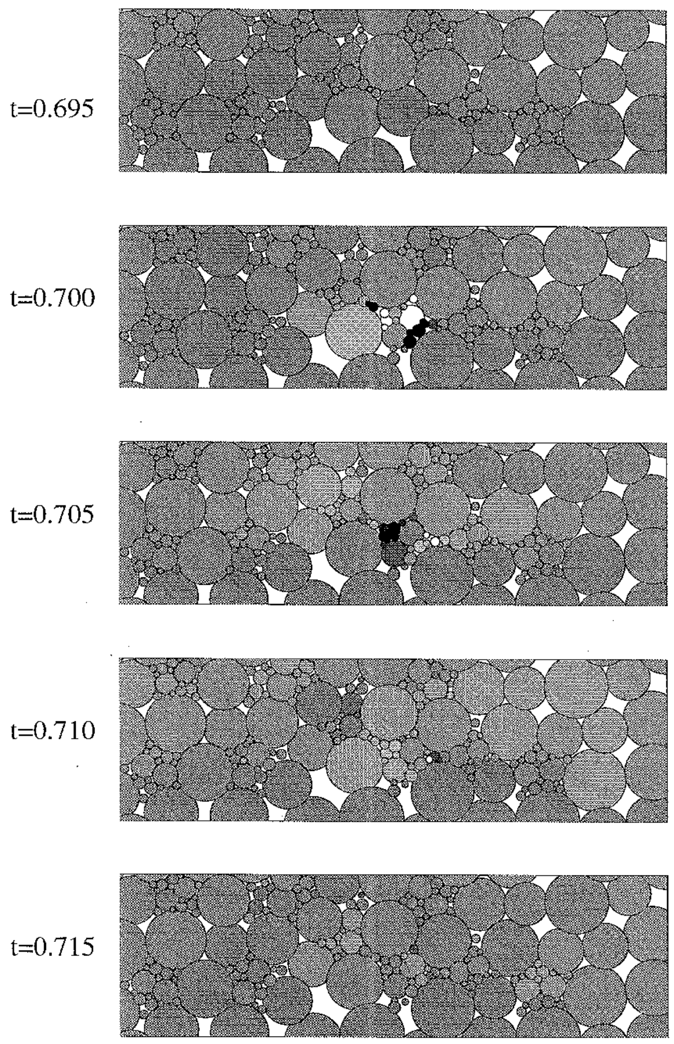

Shearing of polydisperse packing

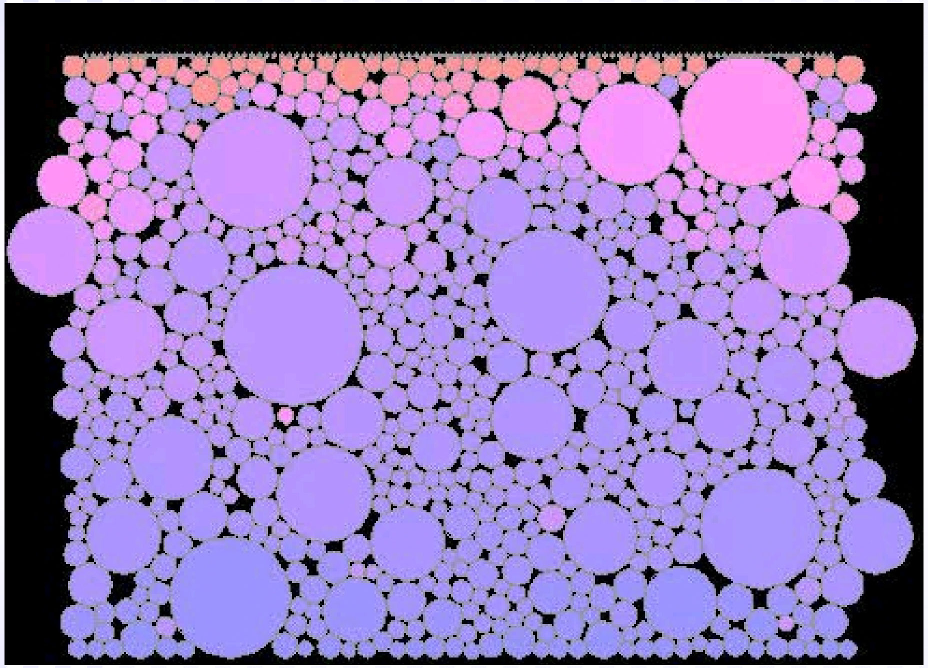

Polydisperse system before shearing

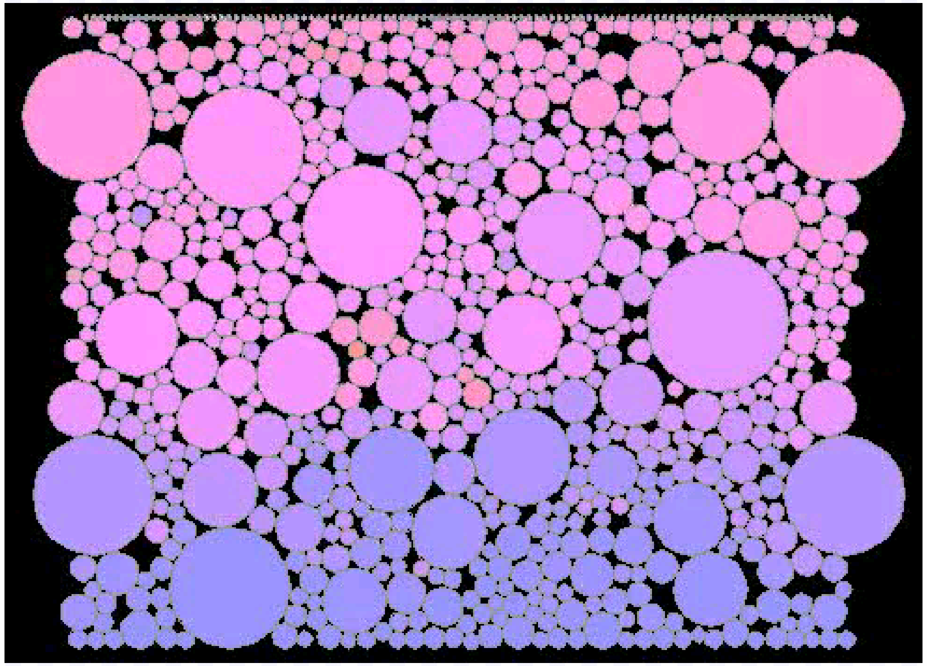

Polydisperse system after shearing

Shearing of bidisperse packing

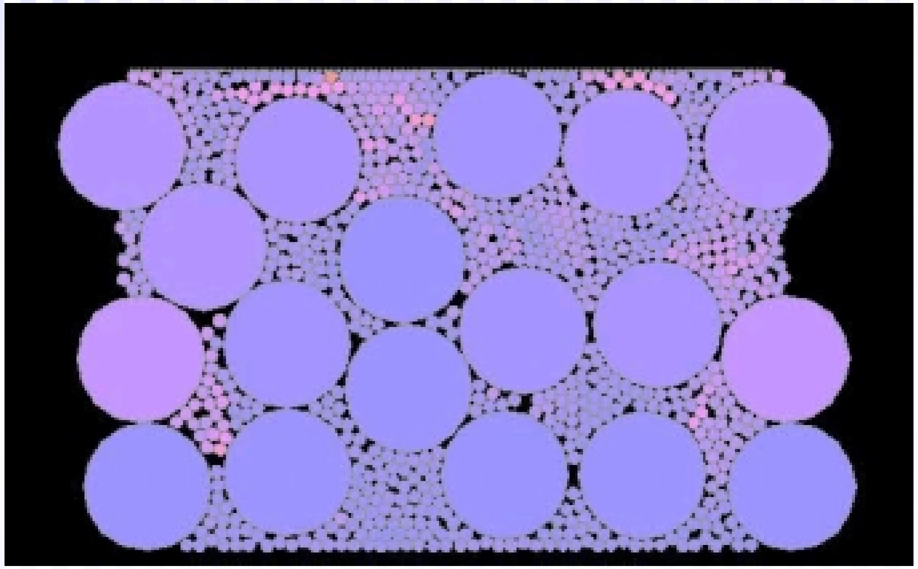

Bidisperse system before shearing

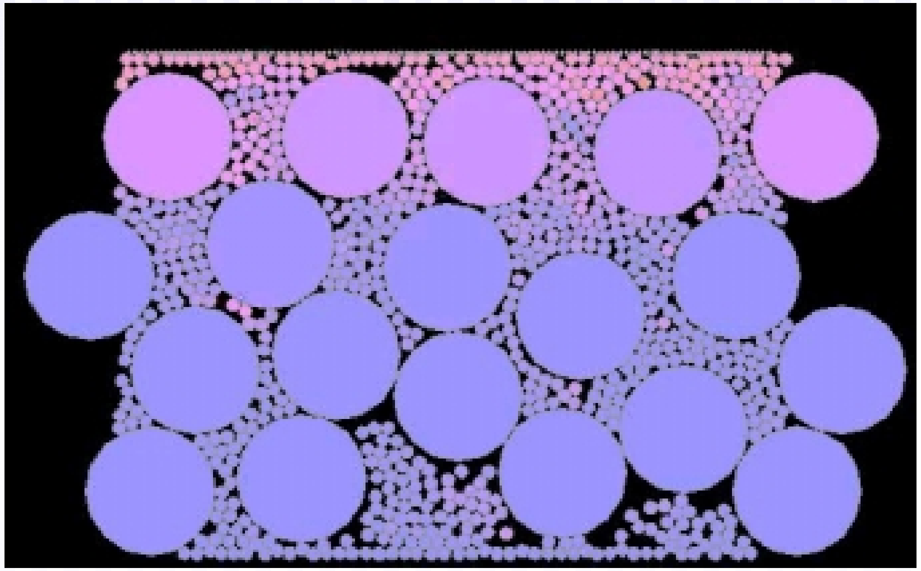

Bidisperse system after shearing

Dilatancy

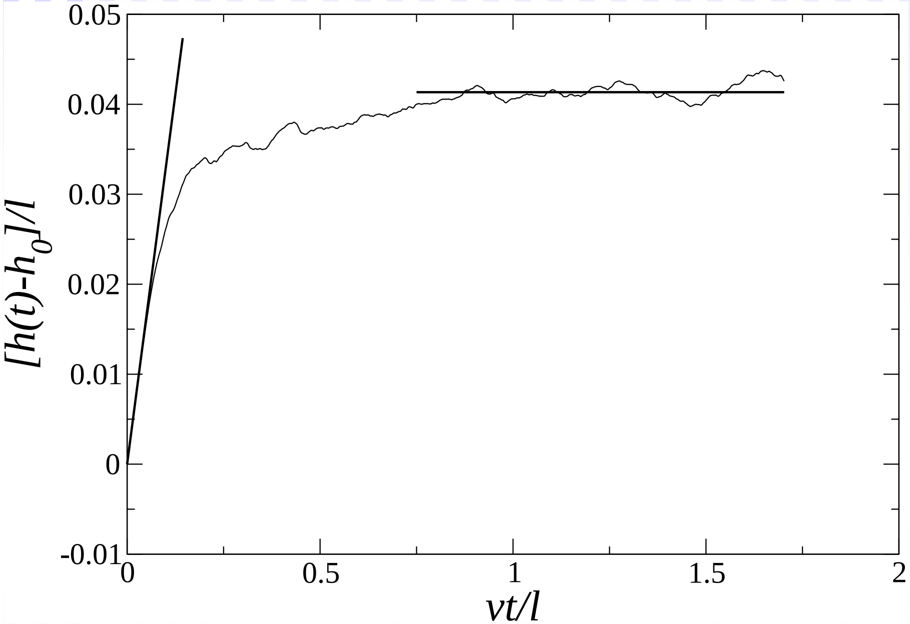

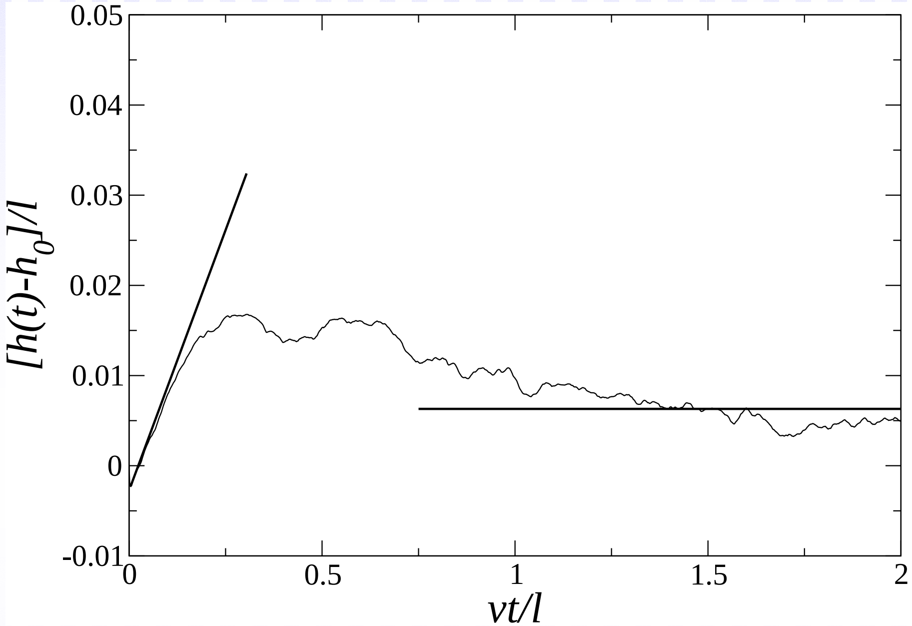

Averaged time series of the change in the height $h(t)-h_0$ as a function of the horizontal displacement ν t of the lid. All distances are given in units of the system size.

First picture: Polydisperse particles with ϕ_0 0.887.

Second picture: Bidisperse particles with R=1/45 and the same value of ϕ_0

In both cases, ν =0.15. Ten simulations were averaged together to obtain these curves. The straight lines show the fits used to obtain Ψ and d_s.

Dilatancy

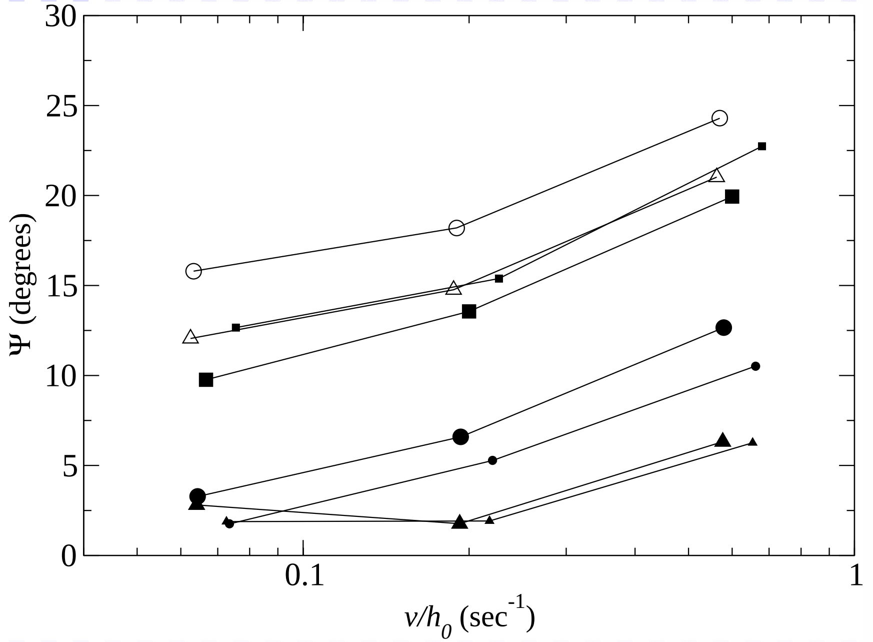

Dilatancy angles Ψ for bidisperse and polydisperse mixtures, as a function of the initial shear rate v/h_0 .

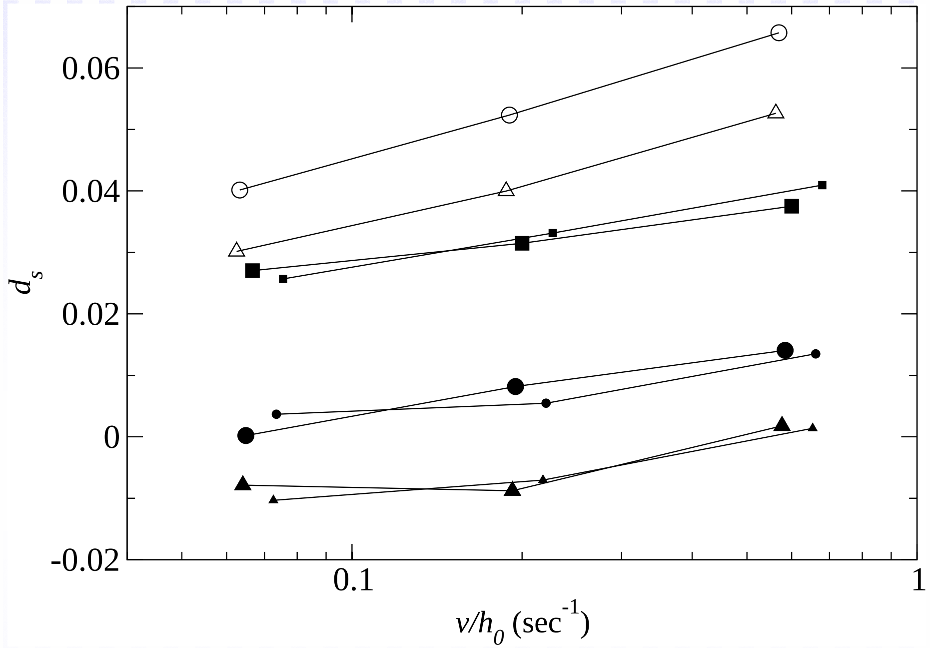

Saturation dilatancy d_s for polydisperse and bidisperse particles.

The empty symbols correspond to polydisperse mixtures; the large, filled symbols correspond to a bidisperse mixture with $R=1/45$, and the small, filled symbols to a bidisperse mixture with $R=1/60$. The squares indicate results for an initial solid fraction $\Phi_0 = 0.911$, the circles $\Phi_0 = 0.887$ and the triangles $\Phi_0 = 0.876$.

Shear force

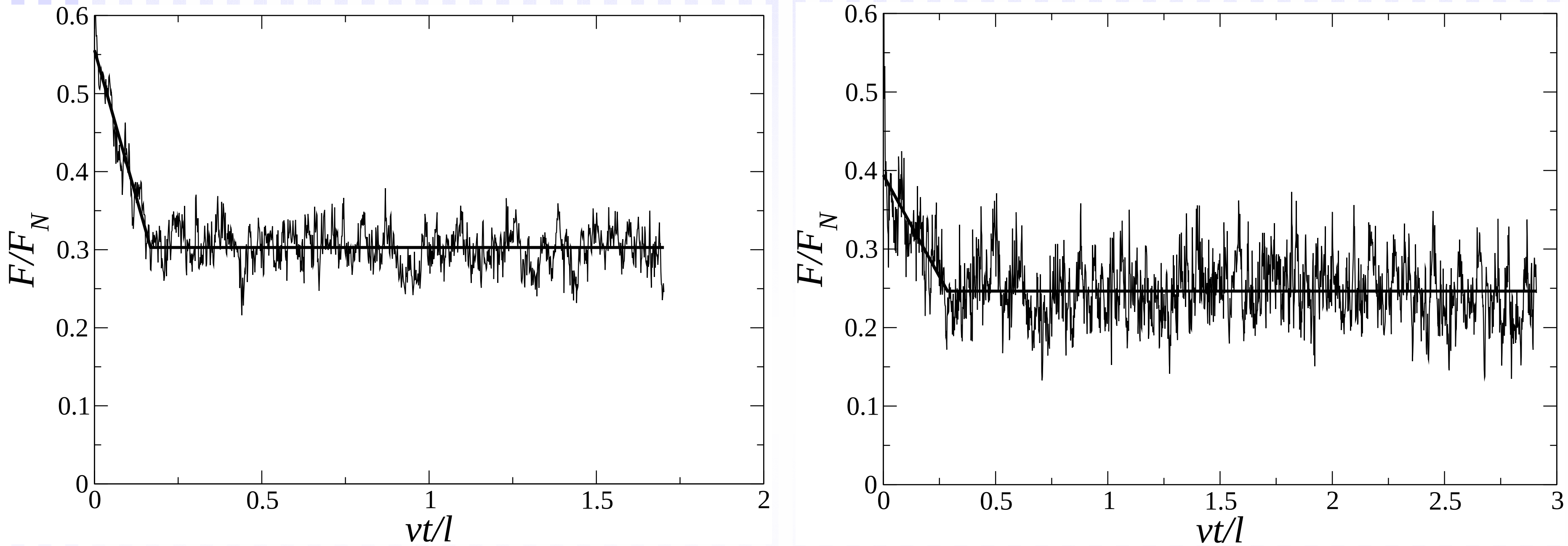

The horizontal force *F(t)* divided by the normal force F_N , as a function of displacement *vt*, for the simulations shown in Fig. 1. First picture: Polydisperse particles with $\Phi_0 = 0.887$ .Second picture: Bidisperse particles with the same value of Φ_0. In both cases, *v* = 0.15. Ten simulations were averaged together to obtain these curves. The straight lines show the fitting of the force.

Local Mohr-Coulomb criterion

- The relation between the volumetric and deviatoric stress at failure is strictly non-linear:

$$\frac{p}{p_r} = \alpha\left(\frac{q}{p_r}\right)^{\beta},$$

- As a consequence, the envelope of all Mohr-Coulomb circles at failure cannot be represented by a single straight line

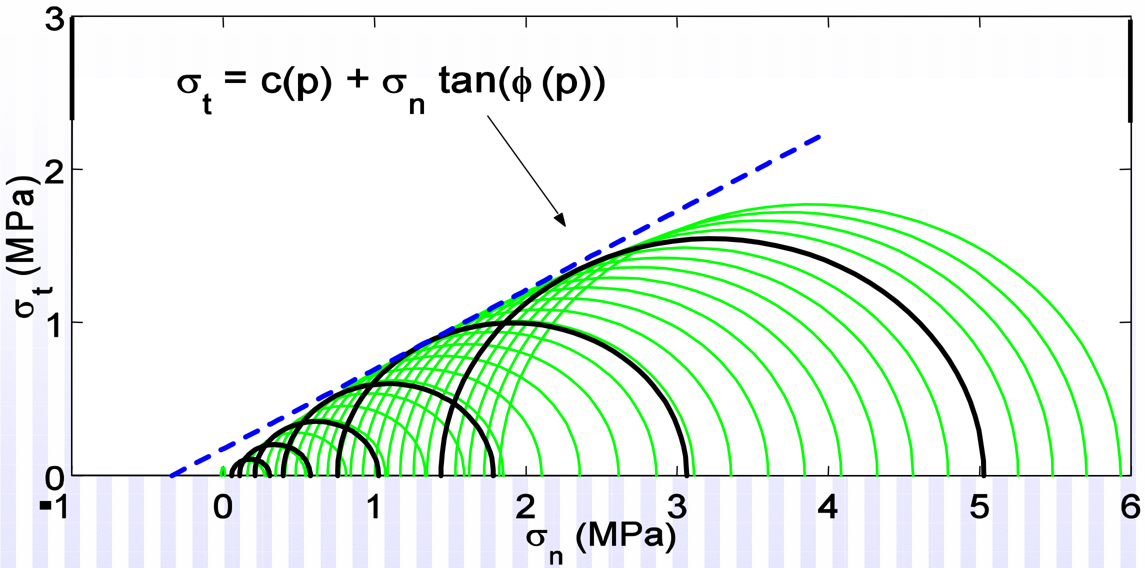

Plastic envelope

- A load-unload stress path for σ_1=2.0·10^5 N/m and σ_3 =1.2·10^5 N/m is followed

- The plastic envelope shows the uni-directional character predicted by elasto-plasticity

- The yield direction does not coincide with the flow direction: non-associated flow rule

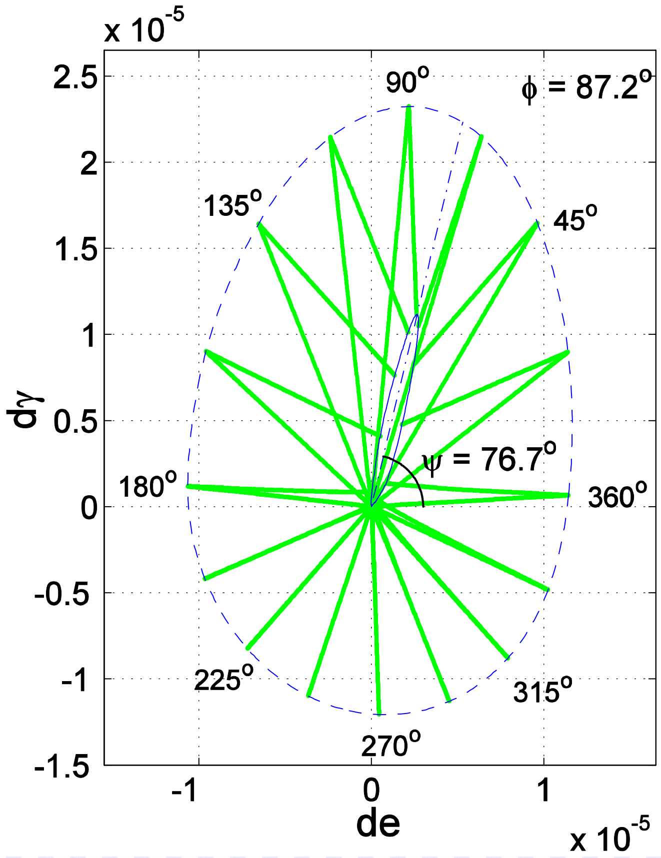

Elastic response

- For $q/p < 0.4$, the envelope responses collapse. Isotropic linear elasticity.

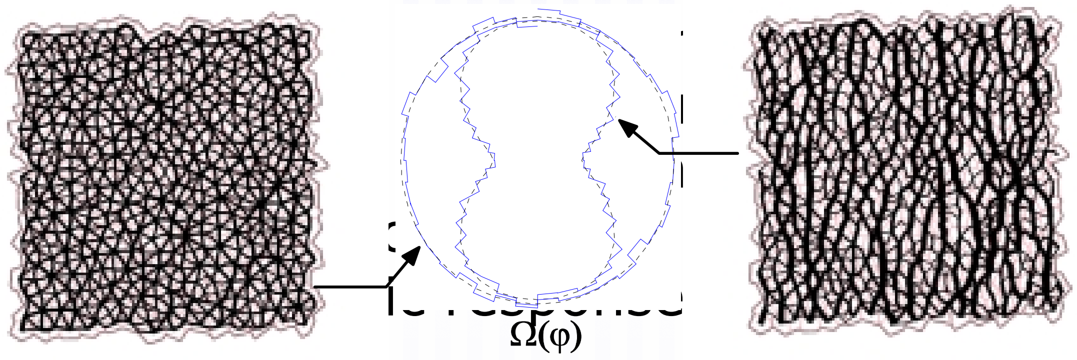

- This anisotropy can be characterized by the distribution of the orientation of the branch vectors: Fabric

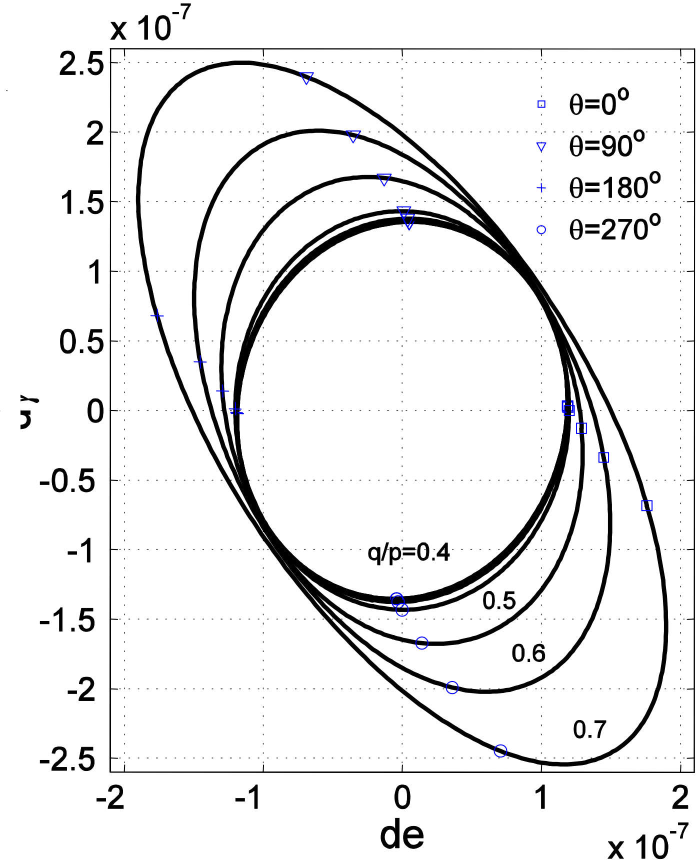

Anisotropy

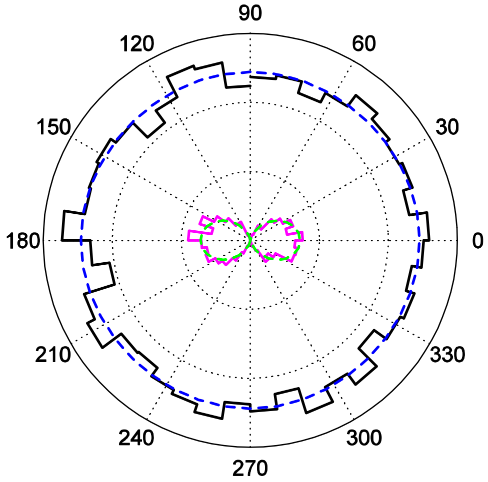

q=0.65p

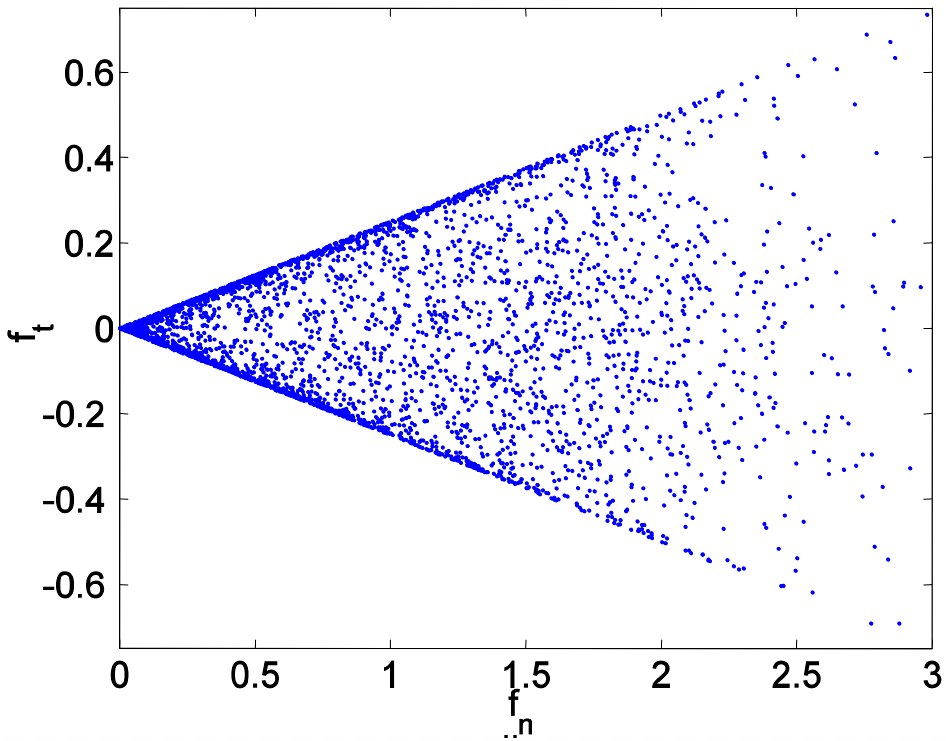

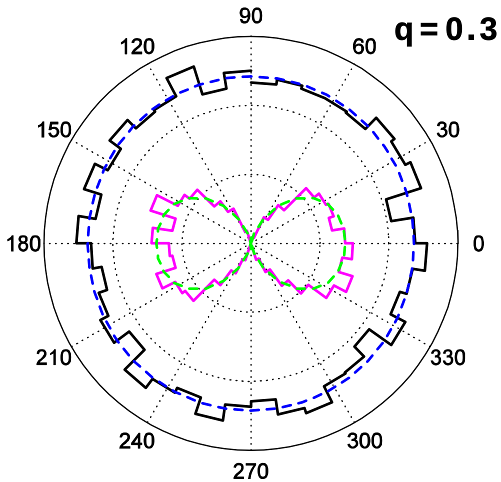

q=0.35p

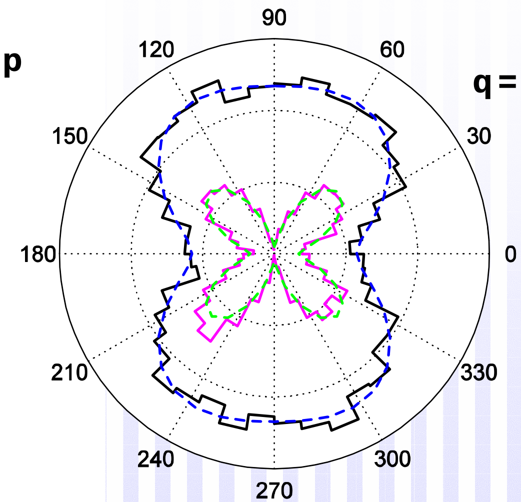

q=0.65p

- The loading intensity changes the contact distribution and induces fluctuation of contact forces

Conclusions

- Future challenges:
  - Three dimensional polyhedra.
  - Realistic grain fragmentation.
  - Non-convex shapes.
  - Anisotropy.
  - Strong polydispersity.
  - Cohesive forces.